

Accepted manuscript doi: 10.1680/jgeot.17.p.185

Submitted: 09 July 2017

Published online in ‘accepted manuscript’ format: 01 May 2019

Manuscript title: Field experiments at three sites to investigate the effects of age on steel piles driven in sand

Authors: R. Carroll*, P. Carotenuto*, C. Dano[†], I. Salama[†], M. Silva[‡], S. Rimoy[§], K. Gavin^{||} and R. Jardine[¶]

Affiliations: *Norwegian Geotechnical Institute, Stryn, Norway; [†]University of Grenoble Alpes, CNRS, Grenoble INP, Grenoble, France; [‡]Universidad Técnica Federico Santa María (formerly Univ. Grenoble Alpes), Chile; [§]University of Dar es Salaam (formerly Imperial College London), United Republic of Tanzania; ^{||}TU Delft (formerly of University College Dublin), Netherlands and [¶]Imperial College London, UK

Corresponding author: R. Carroll, Norwegian Geotechnical Institute, Stryn, Norway. Tel.: +4748847411.

E-mail: roselyn.carroll@ngi.no

ABSTRACT

This paper investigates the influences that steel type, in-situ soil properties, water table depth, pile diameter, roughness and driving procedures have on the ageing behaviour of piles driven in sand. Tension tests have been performed on fifty-one, 48 to 60mm, outside diameter open-ended steel micro-piles driven at well-established research sites at Larvik in Norway, Dunkirk in France and Blessington in Ireland to better understand the processes that control axial capacity set-up trends in the field. Mild steel, stainless and galvanised steel micro-piles were driven and left to age undisturbed for periods of between 2 hours and 696 days before being subjected to first-time axial tension load tests. In addition to reporting and interpreting these experiments, further investigations of the sites' geotechnical profiles are reported, including new piezocone and seismic cone penetration soundings as well as laboratory tests. Integration with earlier ageing studies at the same sites with larger (340 to 508mm outside diameter) open-ended steel piles driven to 7 to 20m embedment's and experiments that varied the piles' initial surface roughness shows that corrosion, pile-scale, roughness, the bonding of soil particles and the driving process can all be highly significant. New insights are gained into the mechanisms that control the axial capacity of piles driven in sand.

Keywords: Model tests; Piles & piling; Sands; Time dependence; Offshore Engineering

INTRODUCTION

Studies of the reliability of conventional design methods' (including the internationally applied API (2011) Main Text method) predictions for the axial capacities of large piles driven in sands have revealed wide scatter and significant bias; see for example Tang et al. (1990) or Jardine and Chow (1996). Alternative methods that offer better reliability include the Fugro-05 (Kolk et al. 2005), ICP-05 (Jardine et al. 2005), NGI-05 (Clausen et al., 2005) and UWA-05 (Lehane et al. 2005a) approaches. All four, which are now cited in API's commentary, employ site-specific CPT profiling to characterise sand state and recognise the effect of the relative pile tip depth (h) on shaft capacity. Independent database studies by Yang et al. (2017) and Lehane et al. (2017) involving high-quality load tests on piles with outside diameters exceeding 0.2m, gave broadly similar results, showing that the "full" ICP-05 and UWA-05 methods for sands offer the lowest degrees of predictive scatter and bias. Field pile driving monitoring has also confirmed that "full" ICP-05 predictions are representative of the shaft capacities developed by large offshore piles within a few days of driving; see Overy (2007) or Jardine et al. (2015).

However, most field load tests are conducted relatively soon after driving and axial capacities change with time. Schmertmann (1991), Åstedt et al. (1992), Chow et al. (1998), Bea et al. (1999), Axelsson (2000), Jardine et al. (2006), Gavin et al. (2013), Karlsrud et al. (2014), Lim and Lehane (2014), Gavin et al. (2015), Rimoy et al. (2015) among others have reported marked growth over weeks and months after driving in sands, although the data are often widely scattered and the processes that control ageing remain uncertain. Ageing appears to benefit shaft capacity primarily (Rimoy et al. 2015) and its effects are clearest in 'first-time' tension tests to failure. Jardine et al (2006), Karlsrud et al. (2014), Rimoy et al. (2015) and Gavin et al. (2015) reported from 'first-time' tension tests on open-ended steel piles (340mm

< OD < 508mm) at three sand sites the systematic trend shown in Figure 1. Capacity growth took place in the first eight months after installation before reaching an upper limiting capacity, around 2.5 times higher than the ICP-05 predictions. The ICP-05 capacities were exceeded within two weeks of driving.

Rimoy and Jardine (2015) and Rimoy et al. (2015) collated ageing data from tests on 103 industrial ($0.2 < OD < 1.3\text{m}$) piles conducted at various ages after driving in sand, as summarised in Appendix A. Most involved multiple re-tests on individual piles after relatively short pauses, so promoting scatter and systematically slower capacity growth trends than are seen in first-time tests (Jardine et al. 2006). The compression capacities include base capacity components that may be of similar, or greater, magnitude to the shaft resistances and may grow as ever larger tip settlements accumulate through re-testing. These factors and a lack of CPT and other site information make the trends harder to interpret than the research outcomes presented in Figure 1. However, the scatter diagrams presented in Figures 2a and 2b from Rimoy et al.'s (2015) datasets of compression tests indicate similar overall set-up trends for concrete and steel piles. Rimoy et al. (2015) also note that: groundwater salinity did not appear to be a key factor; wooden piles set-up in sands; and hard driving reduces short-term axial capacity and provides scope for more marked set-up after installation.

Chow et al. (1998) proposed three mechanisms to explain the effects of age on shaft capacity:

- (i) Stress redistribution leading to higher stationary radial effective stresses σ'_{rc} acting on the shafts,
- (ii) Gains under axially loading of the dilative shaft radial stress $\Delta\sigma'_{rd}$ contribution to capacity demonstrated in instrumented field tests by Lehane et al. (1993) and Chow (1997) and
- (iii) Physiochemical processes involving the soil and shaft.

Gavin et al. (2013) noted that stress redistribution after driving caused the radial effective stress on their instrumented pile to reduce with time. They concluded that the primary mechanism contributing to the ageing of their 340mm outside diameter (OD) steel piles was increased dilative response with time (mechanism ii). A secondary effect involved sand particles bonding to the lower pile shaft, leading to changes in shaft roughness and migration of the shear failure surface into the sand mass (mechanism iii). In contrast Chow et al. (1998) and Jardine et al. (2006) noted the importance of increases in radial effective stresses acting on the pile shaft (mechanism i) to gains in pile capacity.

Jardine and Standing (2012) reported further that low-level cyclic loading enhances capacity. White and Zhao (2006) investigated the impact of environmental or seasonal cycles on pile ageing. They report that the set-up rates of model mild-steel piles increased when water depth was cycled, although stainless steel piles showed no gains with time. Other work suggests that the installation process might also be significant. Lim and Lehane (2014) noted considerably less set-up and 'friction fatigue' with small diameter jacked piles than with piles driven at the same site and argued that ageing involves a recovery process that leads to a stable final upper bound outcome, as seen in the tests summarised in Figure 1.

Rimoy et al. (2015) report intensive long-term calibration chamber testing on 36mm OD, closed-ended, jacked and driven piles in medium-dense silica sand. Their experiments aimed to study the ageing process under closely controlled conditions and included comprehensive measurement of the normal stresses developed on pile shafts and in the sand mass. However, the model piles developed far less set-up than the industrial piles reported in Figures 1 and 2. Imposed cycles of environmental stress change also had little influence on pile capacity. Tsuha et al. (2012) found that low-level cyclic axial loading improved the same model piles' tension capacities while high-level cycling or hard driving severely damaged capacity, as

with industrial piles (Jardine and Standing 2012). Rimoy et al. (2015) suggested that inter-related cyclic and ageing stress re-distribution mechanisms exist that are affected by the bands of fractured and compacted sand that form around steel displacement piles when $q_c > 8\text{MPa}$. Yang et al. (2010) found bands of adhered sand ≈ 5 to $20D_{50}$ thick around their 36mm model piles whose width grew with relative tip depth, h , and amounted to 0.5 to 1.5mm, averaging around $D/30$. Rimoy et al. (2015) argue that the arching mechanism on the outer pile wall may be affected by the ratio of D/D_{50} and that the stress re-distribution mechanism may not apply as effectively to small diameter closed-ended piles.

Growth of either shaft roughness or sand stiffness with age could increase the dilatant $\Delta\sigma'_{rd}$ component of shaft capacity that is captured by the ICP-05 design approach and varies (as proposed by Boulon and Foray (1986)) with $1/D$. Outward radial expansion of the shaft through corrosion reactions could also raise σ'_{rc} while cementing of the fractured sand zone by iron compounds could increase the constant volume interface friction angles, δ_{cv} and could lead, ultimately, to soil-soil shear strength controlling the long term shaft resistance.

This paper reports experiments with fifty-one micro-piles ($48 < D < 60\text{mm}$) driven and tested statically at various ages in tension at the Larvik (Norway), Dunkirk (France) and Blessington (Ireland) sites where the earlier experiments summarised in Figure 1 were conducted. Mild (MS), Stainless (SS) and Galvanised (GS) steel piles were driven above and below the water table under the broadly similar climatic conditions outlined in Table 1. Some piles were installed with smooth and un-corroded surfaces, while others were pre-corroded or pre-driven to modify their surfaces. The experiments investigated how pile material, roughness and diameter affected ageing at three well-characterised research sites with different sand profiles. The piles were left undisturbed during the ageing period. Daily-to-seasonal temperature changes and possibly pore water suction fluctuations above the water table at

Dunkirk and at Blessington were the only environmental variations experienced over the ageing periods. The central questions investigated were:

1. How influential to ageing are any physiochemical processes associated with the pile material, the soil and groundwater?
2. Do other pile-specific factors such as scale, shaft roughness, installation process or environmental site conditions affect the outcomes?
3. Does any upper shaft capacity limit, such as ≈ 2.5 times the ICP-05 medium-term prediction apply, as indicated by Figure 1, irrespective of any continuing active ageing processes?

DESCRIPTION OF TEST SITES

Karlsrud et al. (2014) established NGI's test site, in the Larvik municipality (Norway) around 110km southwest of Oslo, in the Numedalslågen estuary, which has a small tidal range. The ground surface is 2.4m above sea level; 2m of made ground overlies loose-to-medium dense fluvial silty sands and silt layers down to at least 22m. The grain size distributions applying over the study depth range indicate 5 to 20% silt, as presented in Figure 3. Radiocarbon dating indicates deposition 2600 to 1200bp, while XRD testing on a 7.9m deep sample indicates 25% quartz, 37% feldspars and 38% plagioclase and no clay minerals (NGI, 2009). Nine CPT tests within the 15m by 30m test area showed piezocone q_{c-min} and q_{c-avg} consistently around 1 and 2.1 MPa respectively over the 3.5 to 7m depth range, while q_{c-max} showed greater variation (2.8 to 5.5 MPa); see Figure 4(a) and Figure 5. Piezocone excess pore pressures measured at the u_2 position were generally positive and often around 30 kPa (and in some cases 120 kPa); see Figure 4(d). Samples from the boreholes identified in Figure 5 showed the profile becoming siltier at depth; the CPTu results over 20 m depth led Lehane et al. (2017) to exclude the larger Larvik piles from their database of tests in free-draining

silica sands. Ring shear interface and triaxial tests run at Imperial College on borehole samples gave the mechanical parameters listed in Table 2, while the chemical testing results in Table 3 indicate acidic ground water conditions.

The Dunkirk Port-Ouest site described by Jardine et al. (2006), near Gravelines, Northern France, consists of dense-to-very dense marine sand under hydraulic fill derived from the marine sand. The PISA project (Byrne et al., 2015) provided a 25 by 15m area in which 50mm diameter micro-piles were driven to $\approx 2\text{m}$, 2-3m above the water table, within the hydraulic fill; see Figure 6. The test locations were not affected by sea-tides. Grain size distributions are shown in Figure 3; other soil mechanical parameters are summarised in Table 2 and chemical testing is reported in Table 3. The sub-angular particles comprise $\approx 85\%$ silica plus CaCO_3 shell fragments and other minerals that leave the soil slightly alkaline (Chow, 1997). Ring shear interface and triaxial tests run at Imperial College gave the mechanical parameters listed in Table 2; higher ϕ'_p can be expected at $D_r=100\%$ (see Kuwano (1999)). CPT and seismic CPT test investigations performed for the PISA project (Zdravković et al. 2018) and this ageing study provided the representative CPT profiles plotted in Figure 4(b). CPT tests 01, 03 and 04, show q_c increasing from zero to up to 40 MPa at 1.5m depth before reducing significantly. The nineteen PANDA2[®] dynamic penetrometer tests conducted as shown in Figure 6 are not reported in detail but indicated denser conditions in the central test area. Emerson et al (2008) noted that a surface failure mechanism affects the tip resistances developed in shallow CPT tests until a critical depth z_{crit} is exceeded. They propose an expression for z_{crit} which involves CPT diameter, tip resistance and sand unit weight which indicates that near-surface effects probably reduced the q_c values down to 1.5m depth at Dunkirk. Shallower z_{crit} depths are indicated for Larvik which do not affect the CPT profiles applying over the Larvik test piles' 3.8 to 6.2m contact depth range.

The seismic CPT traces plotted on Figure 4(f) indicate relatively high G_{\max} values. Piezocone soundings conducted adjacent to the micro-pile indicated u_2 pore pressures that were generally zero or negative (down to -15kPa) over the depth range of interest, although positive pressures of up to 40 kPa were seen over intervals where fines contents were higher; see Figure 4(e). Suctions of ≈ 10 kPa that may have varied seasonally were found in 'hanging water' laboratory measurements (see Dane and Hopmans 2002) on block samples taken in winter adjacent to the piles. The suction profile interpreted for the PISA programme and shown on Figure 4 (f) was taken as representative in the analyses that follow.

The Blessington site is located 25km southwest of Dublin City. As documented by Gavin and O'Kelly (2007), Gavin et al. (2009) and Doherty et al. (2012), glacial deposition coupled with recent quarrying has left the test location in an overconsolidated state. The water table is ≈ 13 m deep and ground conditions comprise very dense ($D_r \approx 100\%$) glacially deposited medium-to-fine sand composed of quartz and hard limestone (CaCO_3) grains which impart alkalinity to the sand. Figure 3 shows the sand's average grading curve; other mechanical soil properties are summarised in Table 2 while Table 3 provides chemical test results. The pile layout is shown in Figure 7. Eight CPT tests performed within 5m of the micro-piles (Prendergast et al. (2015)) showed average q_c increasing from 10 MPa to 15 MPa at 3m, see Figure 4(c). The Blessington test piles were driven from 1m deep starter holes and the Emerson et al (2008) analysis indicates that the CPT profiles should be mainly free of any shallow-penetration effects. Given the 13m water-table depth, piezocone tests were not undertaken. Water contents are $\approx 11\%$ over the first 2m, where 10 to 12kPa suctions were measured in-situ with Decagon T4 tensiometers with filter lengths between 0.30m and 1.15m. The suctions may vary seasonally, but there are no other significant environmental cyclic actions to consider. Figure 4(g) displays the G_{\max} profile interpreted from Multi-Channel

Analysis of Surface Waves (MASW) reported by Prendergast et al. (2015) and the interpreted in-situ suction.

EXPERIMENTAL PROGRAMME

Piles and installation

Details of the micro-piles tested in this study are summarized in Table 4, while Table 5 (a-c) reports the details of plug formation at the end of pile installation as the final Plug Length Ratios (PLR), defined as the internal plug length divided by the pile embedment depth. Seven 50mm OD Mild Steel (MS) and two 48.2mm OD Stainless Steel (SS) open-ended tubular piles were driven at Larvik to 6.2m tip depth, well below the water table. The piles were driven through cased holes pre-bored to 3.8m depth (see Figure 5), giving an embedment length of 2.4m. Figure 8 A.1 shows the visual condition of the Larvik piles prior to installation. The outsides of the SS piles were air-abraded, and the MS piles were deliberately pre-corroded by 4 months' exposure on-site before driving (with the exception of Pile 2 which was left exposed for some days). Check measurements on spare MS and SS piles that had been exposed for up to a year on site gave average R_{cla} roughness values of 8.5 and 9.8 μm respectively with a Mitutoyo SurfTest-SJ-210-Series-178, that match the typical $R_{cla} \approx 10\mu\text{m}$ of industrial piles (Jardine et al. 2005). The piles were installed by a 0.62 kN weight drop-hammer that could fall between 0.20 and 0.35m and impart energies between 74 to 130 Joules/blow, assuming 60% efficiency. A removable temporary cage inserted in the cased holes ensured pile verticality during installation.

A total of 31 open-ended piles were driven at Dunkirk, as shown in Figure 6, in the southeast corner of the PISA site, 20m from the nearest PISA pile. Multiple roughness measurements with a portable Taylor Hobson Surtronic 25 indicated pre-installation $R_{cla} = 2 \pm 1\mu\text{m}$ for the 21 fresh MS piles (S1 to S20 and S25) and four stainless steel piles (S21, S23, S27 and S29-

Inox) that were driven from ground level in January 2016. An adjustable Sol Solution Grizzly® machine was employed whose maximum energy (475 Joules/blow) and 60 to 70% Energy Ratio is equivalent to that of an SPT hammer. Four of the 21 MS piles were extracted after four months and re-driven as ‘pre-corroded’ rougher piles (R1, R2, R3 and R4). Their rougher shafts and sand adhering to their interiors led to lower Plug Length Ratios (PLR) than with fresh piles. Two of the four SS piles were extracted and air-abraded on their outsides before re-driving in July 2016 as RI5 and RI6. While R_{cla} values were measured before testing for most piles, this was not feasible for MS piles R1 to R4, as their R_{cla} values were higher than the Surtronic 25 could measure, as well as for SS piles R15 and R16. Visual inspection and tactile checks indicated R_{cla} values comparable to those of lightly rusted industrial piles ($\approx 10\mu\text{m}$) for MS piles R1 to R4, while the re-driven shot-blasted SS piles were gauged to have been little affected by the air-abrasion applied and to have retained $R_{cla} \approx 2\mu\text{m}$.

Driving took place in January 2016 at Blessington, with the four pairs of 60mm OD, 4mm thick MS and galvanised (GS) tube-piles shown in Figure 7. The MS piles were mildly pre-corroded. The GS piles’ manufacture involved molten zinc dipping, which left a moderately rough surface; R_{cla} values were estimated as $\approx 10\mu\text{m}$ for both pile types. The top metre of sand was augured to avoid contact with superficial material. Handheld metal post drivers were employed until all piles effectively refused after penetrations of 0.5 to 0.7m. Pile MS1 was damaged and had to be abandoned; a greatly over-sized 4 tonne hammer was employed the next day to achieve the final 2.75m tip depths. While the piles were not exhumed, earlier studies by Gavin et al. (2013) at Blessington indicate that crusts of crushed sand are likely to have formed around the shafts on driving that may have undergone chemical modification during ageing. The mild steel piles are likely to have corroded in-situ.

Testing arrangements

Equipment and procedures varied between sites. The Larvik piles' first-time static tension capacities were measured 1, 14, 21, 78, 189, 315 and 696 days after driving with the system shown in Figure 9. An extension rod connected the pile head, through a load cell, to a suspended hydraulic cylinder actuated by a GDS ADVPC Advanced Pressure/Volume Controller. Jack pressures were raised gradually and held constant for 20 minutes over load stages. A Signal Express Logging system recorded time, load and vertical pile movements relative to the pre-installed casings, which were assumed unaffected by loading. Tests ended when clear load-displacement plateaux developed, and displacements exceeded 7 mm (14% of the piles' OD).

The Dunkirk piles were subject to static tension tests after 0.1, 1, 14, 28, 90, 175, 272 and 315 days' ageing. The reaction frame comprised four steel beams that transferred load to timber foundations; see Figures 10 (a) and (b). An Enerpac manual hydraulic jack acted through a load cell. Load increments were set initially at 10% of the estimated medium-term tension capacity (that reduced as failure approached) and maintained for 15 minutes. Tests continued until displacements reached 15 to 30mm (30 to 60% of pile OD) as measured by two LDVTs supported on vertical stands set 0.7m on either side of the pile axis (Figure 10(a)). A third LDVT measured the loading system deformation and the corrected mean LVDT displacement was applied in test analysis. Strong winds affected displacement measurements in some tests.

The Blessington static load tension tests were carried out 2, 21 and 78 days after driving. The 121-day MS1 pile was abandoned and equipment malfunctioned in the 121-day GS pile test. Testing arrangements were similar to those at Dunkirk, see Figure 11. Displacement measurements relied on a reference beam and three magnetically clamped LVDTs. An

Enerpac manual hydraulic jack applied $\approx 5\text{kN}$ load increments while the LVDTs and the load cell outputs were recorded by a Campbell Scientific Data Logger at 0.1s intervals and transferred to a computer. Load steps were held constant for 30s and tests terminated when it was no longer possible to maintain loads by jacking. The final displacements exceeded 20mm (33% of pile OD). Most tests ended within 10 minutes, while those at Larvik and Dunkirk extended several times longer.

FIELD BEHAVIOUR

Installation

The Larvik piles' driving drop-weight heights increased from 0.2m to 0.35m as penetration advanced, giving the blow-count envelopes and means in Figure 12(a). The final Plug Length Ratios (PLRs) ranged from 0.29 to 0.60, with SS piles showing slightly higher ratios than the pre-corroded MS piles; see Table 5(a).

At Dunkirk the Sol Solution 'Grizzly' machine drove piles S1 to S9 at its maximum (SPT) energy level. Lower ratings (from 21% up to 100%) were applied to other piles to achieve consistent penetration rates and Figure 12(b) presents the blow-count envelopes. The fresh MS and SS piles developed mean PLRs $\approx 43\%$ irrespective of energy levels, while the shot-blasted SS piles' mean PLR was slightly lower (38%) and the pre-corroded MS piles had a significantly lower mean PLR $\approx 22\%$; see Table 5(b).

The Blessington piles required ≈ 90 blows with the post-driving system to achieve initial 0.5m embedment's before effectively refusing to advance. However, as shown in Figure 12(c), only 15-20 further blows were required to complete penetration on the following day with the 4-tonne hammer (falling 200mm) imparting far larger energies (up to 5000 Joules/blow) and developing greater final sets ($\approx 60\text{mm}$, or one diameter/blow) than those (74-to-330 Joules/blow and 5-to-10mm sets) realised at Larvik and Dunkirk. The average PLRs of the

GS piles were lower than for the MS cases (21 and 36% respectively), possibly reflecting higher interior roughnesses for the GS piles; see Table 5(c).

Static load-displacement behaviour

The static test results are summarized in Table 5(a-c) and representative load-displacement curves presented in Figures 13(a-c). The Larvik piles developed ductile plateaux after around 6mm ($\approx 12\%$ of OD), see Figure 13(a). However, the Blessington and Dunkirk piles' displacements at peak-load exceeded the 10% OD limit at which capacities are often defined. The larger piles driven at all three sites required notably smaller normalized displacements to reach tension failure. The resistance of the Blessington and Dunkirk micro-piles' capacities were comparable, and up to 20 times those available in the silty, loose and submerged Larvik sand. The Larvik MS piles showed gains in capacity with time, as well as a tendency for initial stiffness to increase. The Dunkirk MS piles also set-up markedly, but indicated no systematic increase in axial stiffness, mirroring the larger diameter Dunkirk tests; Jardine et al. (2006). The Blessington piles showed little change in capacity or stiffness with age but softened post-peak; the Larvik and Dunkirk piles' responses were ductile.

Shaft capacity trends with time

The micro-piles' peak tension capacities, normalised by those of pre-corroded MS piles at 1 to 2-day age, are presented in Figures 14 (a-c). (The fresh MS and all SS Dunkirk piles had smoother surfaces than the other piles, and the pre-corroded MS Dunkirk piles matched better the Larvik, Blessington and typical industrial pile conditions). Capacities are based on maximum recorded loads corrected for pile and plug weights; no reverse end bearing is considered.

The pre-corroded MS piles driven at Larvik showed, after 315 to 696 days, upper limit capacities ≈ 2.2 times the 1-day reference value. Their set-up factor fell below the equivalent

ratio (≈ 2.9) found from the 508mm OD piles after 200 days; see Figure 1. In contrast to the MS piles, the SS Larvik piles' capacities remained at the pre-corroded MS pile's Day-1 capacity. The apparent test scatter reflects the 'east-end' Piles' 12 and 6 tendencies to plot above the 'west-end' Piles 3, 4 and 5 because the mean CPT q_c values tend to increase by $\approx 15\%$ west-to-east across the test area; the relatively low capacity of Pile 2 reflects its lower period of on-site exposure, pre-corrosion and roughening before driving.

The Dunkirk tests investigated capacity variations between the fresh MS, pre-corroded MS, initially smooth SS and air-abraded SS piles. As shown in Figure 14(b), the fresh MS and the SS piles did not set-up significantly over the first day after driving. However, the capacity of a pre-corroded MS pile tested at 1 day (R1) was 1.5 to 1.8 times higher than that of a relatively smooth fresh MS pile at similar age (S1, S2, S19, S20). Increasing the shaft roughness boosts initial static capacity (and reduce driving PLR) significantly: see Tables 4 and 5(b). The pre-corroded MS and fresh MS Dunkirk piles all developed long-term capacity growth. Despite scatter, the trend lines show steeper (semi-logarithmic) medium-term gains for the fresh MS piles.

It is interesting that the pre-corroded and fresh MS piles both tend towards maxima around 1.4 to 1.6 times the 1-day reference (pre-corroded) capacity. However, the latter ratios are lower than the ≈ 2.2 ratio seen with the Larvik micro-piles and far below the 2.9 to 3.7 gains seen with larger piles at Larvik and Dunkirk respectively: see Figure 1. As at Larvik, the Dunkirk SS piles showed no set-up. The SS piles delivered similar capacities after undergoing air-abrasion, confirming that this treatment had not modified their relatively hard surfaces as significantly as had been intended.

The equivalent trends for Blessington are presented in Figure 14(c). It is noteworthy that the MS or GS piles driven with the 4t hammer developed practically the same capacities and, unlike the larger piles illustrated in Figure 1, no set-up.

Average shaft shear resistances

It is instructive to consider the piles' average failure shaft shear resistance (τ_{avg}) variations with time in Figures 15 (a), (b) and (c). Also plotted in Figure 15 are the τ_{avg} average shaft shear resistances from the larger piles reported in Figure 1 and the average sleeve friction resistance (f_s) over the embedment interval from the closest CPTs, which vary from $\approx 20\text{kPa}$ for Larvik to $\approx 150\text{kPa}$ at Dunkirk and Blessington. Despite the piles' open-ends and the geometrical (h/R^*) or 'friction fatigue' factors identified from instrumented field tests in sands, the pre-corroded rough micro-piles' τ_{avg} resistances exceed or match f_s from day 1 at Dunkirk and Blessington, but only climb towards $0.75 f_s$ after a year at Larvik.

The Larvik MS micro-piles developed markedly lower average resistances at all ages than the equivalent 508mm diameter piles, which may reflect partially the higher CPT q_c values applying over the larger piles' shafts. The opposite applied at Dunkirk where the MS micro-piles developed higher resistances at all ages, despite their shallow depths.

It is interesting that the Blessington micro-piles achieved, in a less variable q_c profile, short-term shaft capacities that matched the long-term upper limit achieved by the large piles and also the average f_s values developed in the monotonically jacked CPT tests. The shaft ageing outcomes found with these relatively long ($L/D = 29.2$) micro-piles are compatible with the hypothesis posed in the introduction that upper limits may apply that cap the shaft resistance, and therefore the radial effective stresses that can develop, despite further corrosion, shaft roughening or any otherwise potentially beneficial ongoing ageing process. The only special

feature of the piles that may have led to their limiting capacities being reached very early after driving was the much higher driving energy, and therefore large penetration for a given blow, imparted by the 4 tonne hammer.

Capacity normalisation

Further insights can be gained by normalising the measured capacities with capacity predictions from design procedures that account for site and pile characteristics. While the Larvik piles were submerged, even small suctions could be important to the Dunkirk and Blessington micro-piles and their σ'_{v0} profiles have been assessed by treating the profiles as if saturated and adding the measured suctions to the total vertical stresses.

The API (2011) Main Text Method assumes that local $\tau_f = \beta \sigma'_{v0}$ where σ'_{v0} is the free field effective stress. An upper-bound τ_f applies to API (2011) that depends (with β) on in-situ relative density and grain size. API (2011) is not applicable to loose sands, so the previous API (1993) version has been applied to the Larvik pile cases. The NGI-05 method uses q_c as the main soil input parameter to determine local relative density, which together with σ'_{v0} controls shaft resistance. The NGI-05 and API Main Text methods do not link τ_f to pile diameter, G or shaft roughness.

The alternative ICP-05 method was developed from field experiments with 102mm diameter instrumented jacked piles, installed to depths of up to 6m in loose dune sand (Lehane et al., 1993) and dense marine sand (Chow, 1997). Local stress sensor measurements of shear and radial stresses plus pore pressures, combined with experiments on larger instrumented open pipe-piles showed that the shaft failures achieved in tension tests conducted within days of installation could be matched by three equations:

$$\tau_f = \sigma'_{rf} \tan(\delta_{cv}) \quad (1)$$

$$\text{with } \sigma'_{rf} \approx (0.8 \sigma'_{rc} + \Delta\sigma'_{rd}) \quad (2)$$

$$\text{and } \sigma'_{rc} \approx 0.029 q_c [\sigma'_{v0}/P_a]^{0.13} (h/R^*)^{-0.38} \quad (3)$$

where τ_f is the local shear stress at failure, δ_{cv} is the ultimate interface shearing angle, h is the depth of the pile tip below the point in question and $R^* = (R^2_{outer} - R^2_{inner})^{0.5}$. Interface ring-shear tests show that δ_{cv} reduces with sand D_{50} and increases with interface average centre line roughness R_{cla} ; Ho et al. (2011). Similar tests on samples from all three sites with appropriate interfaces and stress levels gave the angles indicated in Table 2. The radial effective stress acting on the pile shaft at failure, σ'_{rf} is related to:

- (i) σ'_{rc} the equalised shaft radial effective stress, which depends weakly on σ'_{v0} , increases directly with q_c and reduces with normalised pile tip depth, h/R^* and
- (ii) the change in shaft stress $\Delta\sigma'_{rd}$, due to constrained outward radial movements related to dilation at the interface. Lehane's (1992) and Chow's (1997) review of available field and laboratory model test data for sands indicated that Equation 4 provides suitable estimates for $\Delta\sigma'_{rd}$ when the dilative radial displacement is taken equal to the average peak-to-trough roughness, $2R_{cla}$:

$$\Delta\sigma'_{rd} = 4G R_{cla}/D \quad (4)$$

While $\Delta\sigma'_{rd}$ values are hard to evaluate precisely, Equation (4) indicates that dilation offers relatively modest contributions (often less than 5%) to the medium-term capacities of large diameter industrial piles. However, Axelsson (2000) and Gavin et al (2013), (2015) argue that the 'dilative' term contributes far more significantly to aged industrial piles. It also has the potential to dominate the frictional resistance of micro-piles. While Jardine et al. (2005) suggest a default $R_{cla} \approx 10\mu\text{m}$ estimate for industrial steel piles, the case-specific values

assessed for the present study are summarised in Table 4. Radial movements greater than double the initial R_{cla} could be generated on loading after any corrosion in-situ and/or bonding with sand particles. It is also possible that movements lower than $2R_{cla}$ could apply in any very loose silty/clayey sands that contract when sheared.

The operational (in-situ) sand shear stiffness G is also difficult to select, especially for micro-piles driven above the water table. Jardine et al's (2005) expressions for G_{max} as a function of q_c were applied at Larvik, while the seismic CPT and MASW measurements made at Dunkirk and Blessington provided direct information on the undisturbed in-situ G_{max} profile. The operational values would be raised by the effective stress changes generated by pile installation (particularly at Dunkirk and Blessington), be affected by anisotropy or reduced if the response to shaft loading to failure is non-linear; Jardine et al. (2013). The radial cavity strain ($\delta R/R$) required at the shaft for the sand to unlock from the shaft and allow failure to occur is $4R_{cla}/D$, which amounts to $\approx 0.08\%$ for the rougher micro-piles and exceeds the linear range of most sands. Assuming similar roughness's, the corresponding strains would be up to 10 times lower for the larger piles tested earlier at the same sites.

The ICP-05 approach allows estimates to be made for how driven pile installation and interface dilation affect shaft radial effective stresses. However, the micro-piles are smaller, and involve lower initial effective stresses, than all previous field evaluations of the method and the predictions are inevitably subject to uncertainty.

Tables 2 and 6 list the input parameters considered appropriate for the micro-piles at various test stages and the tension capacities (Q_{sc}) calculated for all three sites. Table 6 also indicates how much of each ICP-05 capacity estimate derives from $\Delta\sigma'_{rd}$ through Equation (4), expressed as a ratio of $\Delta\sigma'_{rd} \tan(\delta_{cv})$ to the total calculated capacity. Table 7 lists the

corresponding average capacities as measured (Q_{sm}) after 1, 85-100 and 175-315 days and gives Q_{sm}/Q_{sc} ratios for the various cases. Figures 16 (a), (b) and (c) plot Q_{sm}/Q_{sc} ratio for each pile tested at the three sites, including the IAC curve from Figure 1.

Considering the loose Larvik sand site first, where 5% to 20% silt contents led to positive excess piezocone pore pressures at some depths (see Figure 4). The early age micro-pile capacities are over-predicted by API (1993) and marginally under-predicted by NGI-05. As noted earlier, the Larvik MS micro-piles showed marked set-up over the months after driving, but to a lesser degree than the large piles shown in Figure 1. ICP-05 predictions made with the default $G-q_c$ function greatly over-predict the micro-piles' initial resistances, giving $Q_{sm}/Q_{sc} = 0.23$, in contrast with the method's more representative prediction for the 508mm Larvik piles short-to-medium term capacities; see Figures 16 (a) and 1. The $\Delta\sigma'_{rd}$ component (see Equation 4) provides 85% of the micro-pile capacity predicted with ICP-05 (see Table 6) and less than 10% for the 508mm diameter cases, so the over-prediction for Larvik must relate primarily to the dilatant term. Although earlier field tests demonstrated highly significant constrained dilation in clean loose sands (Lehane et al. (1993)), a 91% reduction is required in the $\Delta\sigma'_{rd}$ component given by Equation 4 to match the micro-pile capacity seen in the 1 to 2-day tests performed in the loose, silty and contractive Larvik sands.

Moving to the Dunkirk dense sand site, we recall first that applying the criteria proposed by Emerson et al (2008) indicate that the Dunkirk CPT traces may have been subject to near-surface effects down to depths of 1.5m; the latter may also have affected the pile test outcomes. However, the micro-piles' capacities were 9.9 times greater at Day-1 than expected by API (2011) and 1.6 to 1.8 times greater than estimated by ICP-05 or NGI-05.

The SS micro-piles also showed higher capacities than expected, although their Q_{sm}/Q_{sc} ratios

remained fixed at ≈ 1.5 over time. ICP-05 calculations run for closed-ended conditions increased shaft capacity by just 6%, indicating that the micro-piles' relatively low Plug Length Ratios (PLRs) were not the main cause of the discrepancies. Interface constrained dilation and the diameter-dependent $\Delta\sigma'_{rd}$ term (Equation 4) is expected to contribute around half of the shaft capacity and higher-than-undisturbed in-situ operational shear stiffness or shaft roughness again appear to be more likely contributors to the ICP-05's initial under-prediction. The Dunkirk MS micro-piles' capacities grew with age although, as at Larvik, their final relative set-up factors were lower than those earlier with larger (457mm OD) piles shown in Figure 1. The relatively large relative displacements (see Figure 13) required to reach micro-pile shaft failure are consistent with constrained dilation (Equation 4) playing a progressively more significant role over time at Dunkirk. The ultimate capacities of the MS piles lead to ICP-05 Q_{sm}/Q_{sc} ratios that scatter around 2.1 to 2.6, similar to the larger piles' trend, as shown in Figure 16 (b). The roughness of the fresh MS piles is assumed to change with time and R_{cla} is assumed =10 μm after 14 days in-place of the initial 2 μm .

The Blessington micro-piles' capacities amounted to 7.7 times the conventional API (2011) estimate and double the NGI-05 estimate. They are ≈ 2.1 those expected from ICP-05 and remain unchanged with age, falling 15% below the long term ICP Q_{sm}/Q_{sc} ratio of ≈ 2.5 given by the larger piles in Figure 16 (c). If the long-term capacity is subject to an upper limit, as postulated by Jardine et al (2006), Lim and Lehane (2014), Rimoy et al. (2015) and Gavin et al. (2015), this limit appears to have been reached shortly after driving and to have remained unaffected by any subsequent physiochemical or other ageing process. The reasons for this outcome remain open to speculation. However, as noted earlier, the energy used to drive these piles by the 4-tonne hammer advanced the Blessington micro-piles rapidly by a full diameter per blow, in a manner similar to pile jacking. Gavin and O'Kelly (2007) showed

that pile installation resistance at this site is strongly affected by the installation method, with piles installed with long jacking strokes developing shaft capacities close to the f_s values measured in the CPT test. The large axial displacements (up to 30% of OD) required to reach tension failure are compatible with the sand's high δ_{cv} values (see Table 2) and the suggestion that the interface dilation components (Equation 4) of shaft resistance were greater than expected from the ICP-05 calculations.

AGEING MECHANISMS

The micro-pile experiments provide insights on how a range of potential factors affect shaft capacity growth with age.

Cycles in environmental conditions

Considering first the effects of external environmental factors, the absence of set-up for SS or GS piles at any of the three sites demonstrates that diurnal, seasonal or soil micro-structural changes had no independent effect on pile ageing processes.

Physiochemical factors

The physiochemical hypothesis was tested by varying the pile steel materials. Paired MS and SS (or GS) piles driven with similar initial roughness's developed compatible initial capacities that varied between sites, reflecting soil conditions, pile dimensions and roughness's. However, set-up only took place with the MS micro-piles at Larvik and Dunkirk, proving that physiochemical processes were dominant with these small corrodible piles. Although reaction rates may depend on pile surface specific area and condition, ground temperature, chemistry and oxygen supply levels, their resulting impact on capacity appeared to develop at similar overall rates under conditions ranging from the acidic loose, silty and submerged, Larvik sand, to the vadose zone of the dense clean alkaline Dunkirk sand.

Grain scale phenomena close to the pile shafts

Noting that little or no crushing is likely to have developed below the Larvik piles' tips in the low q_c sands present, grain crushing does not appear to have been a necessary condition for the physiochemical ageing processes to apply to the micro-piles or earlier larger (508mm) diameter piles. However, the early-age tests on pre-corroded micro-piles proved that surface roughening provides a significant part of the capacity growth, principally through enhanced dilation. The pre-corroded MS piles consequently showed less capacity growth over time at Dunkirk than initially smooth MS piles, as both tended to similar upper limits.

Corrosion reactions could also cause additional growth in static radial stresses due to expansion of the pile volume as corrosion products crystallise at the shaft. Modification of the shaft as shown in Figure 8 and iron compound cementing also provides a marginally higher effective diameter, probably augmented dilation and δ_{cv} angles that may approach the peak or critical state soil-soil ϕ'_{cs} values. A shift to ϕ'_{cs} would offer a $\tan\phi'_{cs}/\tan\delta_{cv}$ capacity contribution which might provide an additional $\approx 25\text{-}35\%$ in silica sands for piles of any diameter.

Enhanced dilation under loading

Instrumented field tests show that constrained dilation under loading contributes to shaft capacity in sands. Axelsson (2000) and Gavin et al (2013) observed that it contributed to capacity growth over time with industrial concrete and steel driven piles. The shapes of the Dunkirk MS micro-piles' load-displacement curves also indicate that interface dilation became more important with time. However, no set-up or displacement to failure growth applied to the SS and GS micro-piles, so physiochemical processes involving mild steel (or concrete) are required to generate any additional radial movements that might contribute to

raising the shaft stresses in combination with any shift from the interface shear angle rising from δ_{cv} towards ϕ'_{cs} .

Evidence obtained by comparing piles with different diameters

Set-up appears to be diameter-dependent: the micro-piles all developed lower relative gains than the larger piles tested earlier at the same site. The corrosion reactions observed around the pile shafts can be expected to advance at rates that are independent of the piles' diameters. Micro-piles and larger industrial piles can therefore be expected to show similar absolute gains in effective diameter and absolute additional radial movements due to dilation when loaded to failure. The relative impact of these changes on shaft capacity should all diminish with increasing pile diameter, as indicated by Equation 4, rather than follow the opposite trend seen in the field experiments. Recalling from Figure 2(a) that industrial concrete piles also set-up and that capacity gains have been observed over relatively short times with offshore piles driven in sands to penetrations where the oxygen supply is severely limited (Jardine et al. (2015)) it appears that steel corrosion cannot be the only process at work. Other factors must be operating whose impact is greater with larger diameter piles.

Radial stress redistribution

It remains highly challenging to undertake analyses of installation in sand that explore the generated in-situ stress fields quantitatively. However, Yang et al. (2014) and Zhang et al. (2014) show that an arching stress field can be expected to develop in sands around even monotonically penetrating piles. The SS and GS micro-pile experiments confirm Rimoy et al.'s (2015) postulate that radial stress redistribution does not contribute significantly to micro-pile ageing. However, the redistribution mechanism may be more effective around larger open-ended driven piles which involve higher: (i) initial stresses, (ii) ratios of diameter D to crushed-sand bandwidth, (iii) D to wall thickness, t , ratios, (iv) final PLRs and (v) total

blow-counts. The grain crushing, dynamic load cycling and shear band formation that take place when industrial piles with high D/t ratios are driven may all accentuate arching around the shaft and provide greater scope for stress redistribution and capacity growth over time and contribute to the set-up observed shortly after driving (in significant water depths) for large offshore piles in dense sands.

Pile driving technique

It has been argued that the lack of set-up, even by physiochemical processes, of the MS Blessington piles was related to employing an oversized hammer over their main drive lengths, which led to installation conditions similar to pile-jacking with penetrations of one full diameter per blow and contrasted strongly with the conventional driving of the 340mm OD piles, which manifested the strong set-up seen in Figure 1. Other tests at Blessington by Chatta (2006) on 73 mm OD closed-ended piles installed with both 1m and 50mm jack strokes and tests with 75, 100 and 114 mm OD open-ended piles driven (with high blow counts) by an SPT hammer (Gavin et al. (2003)) confirm that installation procedure affects both PLRs and short-term capacity. Hard driving reduces the radial effective stresses around the shaft and leaves greater scope for capacity growth than the micro-piles' high-energy installation, which delivered unusually high short-term capacities that fell close to the upper-limits suggested by Figures 1 and 16.

Possible upper limit to aged shaft capacities

The tests at all three sites support the hypothesis that an upper limit applies to aged shaft capacity which amounts to 2.1 to 2.5 times the ICP-05 predictions, irrespective of any ongoing ageing process.

CONCLUSIONS

Fifty-one co-ordinated static first-time tension tests have been reported, along with site investigations, on open-ended steel micro-piles failed at ages between 0.1 and 696 days, at sand sites covering loose-to-dense conditions and varying silt contents. Fresh smooth, and pre-corroded rough, mild steel, stainless and galvanised steel piles were considered.

Integration with earlier larger diameter pile tests and an independent database study allowed investigation of how pile diameter, steel corrodibility, surface roughness and ground conditions affect ageing behaviour. The influence of driving procedure was also considered.

Reflecting the key questions posed in the introduction, three groups of conclusions are drawn:

1. Pile material, roughness and physiochemical processes were found to be highly influential to ageing:
 - a. Physiochemical processes dominated the marked set-up shown by mild steel micro-piles in submerged silty-loose (Larvik) sand and clean-dense unsaturated (Dunkirk) sand.
 - b. No set-up was seen with non-corrodible stainless or galvanised steel piles, so no independent ageing process, such as radial stress re-distribution, growth of shear stiffness, dilation due to creep or enhanced grain interlocking affected the micro-piles significantly in the absence of physiochemical effects.
 - c. The physiochemical processes identified as potentially affecting ageing include: (i) pile surface roughness increasing through redox reactions, (ii) bonding between sand and corroding shaft, (iii) marginally higher effective diameters, (iv) interface shear angles rising towards the ϕ'_{cs} limit and (v) growth in static radial stress σ'_{rc} due to radial expansion of the corroding steel.

- d. However, the database studies outlined in Figure 2 and Appendix A show that concrete and steel piles with diameters between 0.2 and 1.3m gain capacity at similar rates over time. Steel corrosion reactions cannot be the only mechanism that leads to set-up with larger piles driven in sands.
 - e. Pile roughness and constrained dilation had a critical effect on the micro-piles' capacities.
2. Four further key points emerged concerning the specific piles and sites investigated:
- a. The mild steel micro-piles developed lower set-up factors than the larger industrial piles tested previously at the Larvik, Dunkirk and Blessington test sites.
 - b. The lack of set up shown by stainless steel piles proved that seasonal variations in temperature and/or possibly pore pressures had no independent influence on pile ageing, which also appeared largely independent of the sites' initial geochemical conditions.
 - c. The micro-pile shaft capacity measurements indicate that the ICP-05 dilation term expressed in Equations 2 and 4 gives only an approximate indication of the observed field behaviour. While the impact of dilation is minor for large piles at early ages after driving, the discrepancies are important with micro-piles.
 - d. The ICP-05 dilation term should be set to zero when assessing short-to-medium term shaft capacities in loose silty sands that manifest positive piezocone pore pressures.

- e. Equally, applying Equation 4 as recommended in ICP-05 appears to underestimate significantly the contribution that constrained dilation makes to micro-pile shaft capacity in dense sands.
 - f. Short-term capacity and set-up depend on the installation process. A range of tests conducted earlier at Blessington confirmed that heavy driving reduces the radial effective stresses available after installation and creates scope for capacity gains over time. However, employing a greatly over-sized hammer for the micro-piles led to capacities that did not change with time and were close at an early age to the upper limit developed after long ageing by conventionally driven piles.
3. Considering, the third key question as to whether any upper limit applies to shaft capacity, irrespective of any continuing active ageing processes:
- a. Upper-limits to shaft capacity were found at all three sites, by piles of two scales, that appeared to fall around 2.1 to 2.5 times the capacities estimated by the medium-term ICP-05 procedures when based on best estimates of pile and soil conditions.
 - b. While most piles are installed with initial capacities well below this upper limit, a range of ageing processes apply in the field that allow growth over time towards the site-specific maxima, which appear to be controlled by limits to the radial pressures that can be developed around the pile shafts.
 - c. Exceptions to the above general trend include (i) chemically inert stainless steel micro-piles driven in dense Dunkirk sands which showed no set-up above their initial capacities that fell around 50% above the ICP estimates (ii) the micro-piles driven in loose, silty and contractant Larvik sand, whose degrees

of interface dilation and therefore shaft capacities fell far below those expected.

Acknowledgements

The financial contributions of Norwegian Research Council and NGI to the field tests at Larvik are acknowledged, as are Axel Walta's and other NGI colleagues' technical contributions and permission to test at the site from Larvik Kommune. Testing at Dunkirk was conducted by the Grenoble 3SR laboratory and permissions from the Port Autonome of Dunkirk, the PISA project and Orsted to access the site are gratefully acknowledged, as are technical and scientific contributions from Sol Solution regarding pile installation and site investigation. The authors also would like to sincerely thank Grenoble 3SR laboratory students who contributed to the experimental campaign: M. Del Genio and O. Moreno. The contributions of Luke O'Doherty and Dr. Luke Prendergast to the UCD field tests at Blessington are acknowledged, as are earlier contributions from Dr. David Igoe and Dr. Lisa Kirwan. Roadstone limited are gratefully acknowledged for permission to use their quarry at Blessington. Tingfa Liu, Huarong Chen and Santiago Quinteros are also thanked for their contributions to supporting interface shear and triaxial tests conducted at Imperial College.

NOTATION LIST

D	pile outer diameter
D_r	relative density
D_{50}	size of particle at 50% point on particle distribution curve
D_{90}	size of particle at 90% point on particle distribution curve
f_s	sleeve friction resistance in CPT and CPTU
G	operational shear modulus
G_{\max}	small strain shear modulus
h	depth of the pile tip below the point in question along the pile
q_c	measured cone resistance in CPT and CPTU
Q_c	compression capacity
Q_s	tension shaft capacity
Q_{sc}	calculated tension shaft capacity
Q_{sm}	measured tension shaft capacity
R^*	equivalent pile radius for open-ended piles
R_{cla}	centre-line average roughness
t	pile wall thickness
u_2	pore pressure measured behind the cone in CPTU
z_{crit}	critical depth for shallow CPT
δ_{cv}	constant volume interface shearing angle
$\delta R/R$	radial cavity strain
$\Delta\sigma'_{rd}$	change in radial shaft stress during loading
σ'_{rc}	equalised shaft radial effective stress on the pile shaft
σ'_{rf}	radial effective stress on the pile shaft at failure
σ'_{v0}	in-situ effective stress
τ_{avg}	piles' average shaft shear resistance at failure
τ_f	local shear stress at failure
ϕ'_{cv}	constant volume angle of shearing resistance
ϕ'_p	peak angle of shearing resistance

Appendix A

Pile ageing in silica sands: Case studies identified by Rimoy et al (2015).

Reference	Site location	Ground description	Pile description				Load test description
			Material (Number of piles)	Average length (m)	Section/ **Diameter (m)	L/D	Type, Direction
							D/S*, C/T*
Tavenas & Audy (1972)	St Charles River, Quebec City, Canada	Medium uniform sand	Concrete (28)	11	Hexagonal 0.305	36	S, C
Skov & Denver (1988)	Hamburg, Germany	Sand and silt	Concrete (6)	21	Square 0.395	53	D/S, C
	Südkaai, Hamburg Harbour, Germany	Coarse medium to medium fine sand and fine gravel	Steel (1)	33.7	Pipe 0.762	44	D/S, C
Seidel et al. (1988)	Australia	Loose to dense sand	Concrete (1)	11	Square 0.508	21	D/S, C
Zai (1988)	China	Fine sand	Steel (5)	41.4	Pipe 0.609	68	D, C
DiMaggio (1991)	Mobile County, Alabama, USA	Saturated silty sand	Concrete (5)	21.5	Square 0.688	31	D/S, C
Svinkin et al. (1994)	Various sites, USA	Silty clayey fine sand	Concrete (1)	38	Square with void 0.573	66	D/S, C
			Concrete (1)	27.4	Square	68	

Reference	Site location	Ground description	Pile description				Load test description
			Material (Number of piles)	Average length (m)	Section/ **Diameter (m)	L/D	Type, Direction
							D/S*, C/T*
					0.402		
			Steel (1)	25.3	Closed ended pipe 0.324	78	
York et al. (1994)	JFK International Terminal, Jamaica, New York, USA	Organic silty clays and peats underlain by fine to medium glacial sand	Steel (13)	19.9	Open ended 0.355 tapered to 0.2 over 7.6m	99.5	D/S, C
			Timber (1)	15.8	N/M	N/A	
			Steel (1)	20.7	Pipe	N/A	
Chow et al. (1998)	Port Autonome de Dunkerque, Dunkerque, France	Medium to dense marine silica sand q_c average 21MPa	Steel (2)	16.5	Open ended pipe 0.324	51	D/S, C/T
Axelsson (2000)	Fittja Strait, Vårby, Stockholm, Sweden	Loose to medium dense glacial sand. q_c 2 - 8MPa, < 50% silica	Concrete (4)	17.4	Square 0.265	65.8	D/S, C
Fellenius	JFK	Fine to	Steel (1)	18	Open	40	D, C

Reference	Site location	Ground description	Pile description				Load test description
			Material (Number of piles)	Average length (m)	Section/ **Diameter (m)	L/D	Type, Direction
							D/S*, C/T*
& Altae (2002)	International Terminal, Jamaica, New York, USA	coarse medium dense to dense glacial sand			Monotube 0.45		
			Steel (1)	18	Open tapertube 0.45 – 0.2 over 7.6m	90	D, C
Jardine et al. (2006)	Port Autonome de Dunkerque, Dunkerque, France	Medium to dense marine silica sand q_c 20MPa	Steel (3)	19.02	Open ended pipe 0.457	41.6	S, T
Rimoy (2013)	Red Sea port development	Dense coral granitic gravels & sands with cementation	Steel (13)	31.8	Open ended pipe 1.219	26.1	D/S, C
Gavin et al. (2013)	Blessington, Ireland	Dense fine glacial sand; q_c 10 - 20MPa	Steel (4)	7	Open ended pipe 0.34	20.6	S, T
Karlsrud et al. (2014)	Larvik, Norway	Loose to medium dense clayey silty fine sand	Steel (7)	21.5	Open ended pipe 0.508	42.3	S, T
	Ryggkollen, Norway	Medium dense medium	Steel (6)	20	Open ended pipe	49.3	S, T

Reference	Site location	Ground description	Pile description				Load test description
			Material (Number of piles)	Average length (m)	Section/ **Diameter (m)	L/D	Type, Direction
							D/S*, C/T*
		fine to coarse sand with cobbles			0.406		

*C: Compression, T: Tension, D: Dynamic testing with PDA and analysed by CAPWAP (Rausche et al. 1985), S: Static testing, N/M: Not Mentioned.

Further comments on the case studies:

- 1) **For piles with non-circular cross-sections the diameter of an equivalent circular cross-section base area is used
- 2) Tavenas & Audy's (1972) aged piles capacities were obtained from Fig. 15 of the reference

REFERENCES

- Aghakouchak, A., Sim, W.W. and Jardine, R.J. (2015) Stress-path laboratory tests to characterise the cyclic behaviour of piles driven in sands. *Soils and Foundations*, 55(5), 917-928.
- API (1993) "Recommended Practice for Planning, Designing and Constructing Fixed Offshore Platforms – Working Stress Design" API RP 2A-WSD, 20th Edition, 1 July 1993
- API (2011) Geotechnical and foundation design considerations. Recommended Practice 2GEO. Report.
- Åstedt, B., Weiner, L. & Holm, G. (1992) Increase in bearing capacity with time for friction piles in silt and sand. In: *Proceedings of Nordic Geotechnical meeting*, Aalborg, Denmark, 411-416.

Attwooll, W. J., Holloway, D. M., Rollins, K. M., Esrig, M. I., Sakhai, S. & Hemenway, D.

(1999) Measured pile set-up during load testing and production piling: I-15 corridor reconstruction project in Salt Lake City, Utah. Transportation Research Record.

Journal of the Transportation Research Board, 1663(99-1140), 1-7.

Axelsson, G. (2000) Long-term set-up of driven piles in sand. PhD thesis, Royal Institute of Technology, Stockholm, Sweden.

Bea, R. G., Jin, Z., Valle, C. & Ramos, R. (1999) Evaluation of reliability of platform pile foundations. journal of geotechnical and Geoenvironmental Engineering, ASCE, 125(8), 696-704.

Boulon, M. & Foray, P. (1986) Physical and numerical simulation of lateral shaft friction along offshore piles in sand. In: In Proceedings of the 3rd International Conference on Numerical methods in Offshore piling, Nantes, France Editions Technig, Paris, France, 127-148.

Bullock, P. J., Schmertmann, J. H., McVay, M. C. & Townsend, F. C. (2005) Side shear setup. I: Test piles driven in Florida. Journal of Geotechnical and Geoenvironmental Engineering, ASCE, 131(3), 292-300.

Byrne, B. W., McAdam, R., Burd, H. J., Houlsby, G. T., Martin, C. M., Zdravković, L., Taborda, D. M. G., Potts, D. M., Jardine, R. J., Sideri, M., Schroeder, F. C., Gavin, K., Doherty, P., Igoe, D., Muir Wood, A., Kallehave, D. & Skov Gretlund, J. (2015) New design methods for large diameter piles under lateral loading for offshore wind applications. In: Proceedings of the 3rd International Symposium on Frontiers in Offshore Geotechnics (ISFOG), Oslo, Norway: Taylor and Francis Group, 1, 705-710.

- Chatta, I. (2006) Investigation of installation effects and cyclic loading on piles in sand. MS Thesis, University College Dublin.
- Chow, F. C. (1997) Investigations into displacement pile behaviour for offshore foundations. University of London (Imperial College), London, UK.
- Chow, F. C., Jardine, R. J., Bruzy, F. & Nauroy, J. F. (1998) Effects of time on capacity of pipe piles in dense marine sands. *Journal of Geotechnical and Geoenvironmental Engineering*, ASCE, 124(3), 254-264.
- Clausen, C. J. F., Aas, P. M. & Karlsrud, K. (2005) Bearing capacity of driven piles in sand, the NGI approach. In: *In Proceedings of 1st International Symposium on Frontiers in Offshore Geotechnics*, Perth, Australia: Balkema, 547-580.
- Dane, J.H., and J.W. Hopmans. (2002) Soil Water Retention and Storage - Introduction. IN: *Methods of Soil Analysis. Part 4. Physical Methods.* (J.H. Dane and G.C. Topp, Eds.). Soil Science Society of America Book Series No. 5. Pages 671-674
- DiMaggio, J. (1991) Dynamic pile monitoring and pile load test report. Demonstration project No. 66, 1-165(2), Mobile County, Alabama, FHWA, USA.
- Doherty, P., Kirwan, L., Gavin, K., Igoe, D., Tyrrell, S., Ward, D. & O'Kelly, B. C. (2012) Soil properties at the UCD geotechnical research site at Blessington. In: *Proceedings of the National Bridge and Concrete Research in Ireland Conference.*, Dublin, Ireland, 499-504.
- Emerson M., Foray P., Puech A. and Palix E (2008). A global model for accurately interpreting CPT data in sands from shallow to greater depth., *Geotechnical and geophysical site characterization: Proceedings of the Third International Conference on Site Characterization ISC'3* (pp. 687-694). Taipei: Taylor& Francis, London.

Fellenius, B. H. & Altaee, A. (2002) Pile Dynamics in Geotechnical Practice-Six Case

Histories. In: Int. Deep Found. Congress, An International Perspective on Theory, Design, Construction, and Performance. Orlando, USA. ASCE Geotechnical Special Publication 116, 2, 619-631.

Gavin, K.G. and Lehane, B.M (2007). Base Load-Displacement Response of Piles in Sand, Canadian Geotechnical Journal, Vol. 44, No. 9, September 2007, pp 1053-1063.

Gavin, K. G. & O'Kelly, B. C. (2007) Effect of friction fatigue on pile capacity in dense sand. Journal of Geotechnical and Geoenvironmental Engineering, ASCE 113(1), 63-71.

Gavin, K. G., Lehane, B. M. & Prieto, C. (2003) The development of skin friction on pipe piles in overconsolidated sand. In: Proc. XIII ECSMGE, Prague, 2.

Gavin, K., Adekunle, A. & O'Kelly, B. (2009) A field investigation of vertical footing response on sand. Proceedings of the Institution of Civil Engineers-Geotechnical Engineering, 162(5), 257-267.

Gavin, K., Igoe, D. & Kirwan, L. (2013) The effect of ageing on the axial capacity of piles in sand. Institute of Civil Engineers Proceedings Geotechnical Engineering, 166(2), 122-130.

Gavin, K., Jardine, R. J., Karlsrud, K. & Lehane, B. M. (2015) The effects of pile ageing on the shaft capacity of offshore piles in sand. Keynote paper. In: Proceedings of the 3rd International Symposium on Frontiers in Offshore Geotechnics (ISFOG), Oslo, Norway: Taylor and Francis Group. 1, 129-152.

Ho, Y.K., Jardine, R.J and Anh-Minh, N. (2011) Large displacement interface shear between steel and granular media. Géotechnique, 61(3), 221-234.

Holeyman (2012) Essais de chargement dynamique sur Pieu B-2 de Loon-Plage SOLCYP.

In: UCL, GeoMEM presentation at the SOLCYP meeting, Paris, France (in French)

Jardine, R.J. and Chow, F.C. (1996) New design methods for offshore piles. MTD

Publication 96/103, MTD, London.

Jardine, R. J. & Standing, J. R. (2012) Field axial cyclic loading experiments on piles driven in sand. *Soil and Foundations*, 52(4), 723-736.

Jardine, R. J., Chow, F. C., Overy, R. F. & Standing, J. R. (2005) ICP design methods for driven piles in sands and clays. London, UK: Thomas Telford.

Jardine, R. J., Standing, J. R. & Chow, F. C. (2006) Some observations of the effects of time on the capacity of piles driven in sand. *Géotechnique*, 56(4), 227-244.

Jardine, R. J., Zhu, B. T., Foray, P. & Yang, Z. X. (2013) Interpretation of stress measurements made around closed-ended displacement piles in sand. *Géotechnique*, 63(8), 613-627.

Jardine, R.J., Thomsen, N.V., Mygind, M., Liingaard, M.A. and Thilsted, C.L. (2015) Axial capacity design practice for North European Wind-turbine projects. Proc. International Symposium Frontiers in Offshore Geotechnics (ISFOG), Oslo, CRC Press, London, 1, 581-586.

Karlsrud, K., Jensen, T. G., Wensaas Lied, E. K., Nowacki, F. & Simonsen, A. S. (2014) Significant ageing effects for axially loaded piles in sand and clay verified by new field load tests. In: Proceedings of the Offshore Technology Conference, Houston, TX, USA, OTC-25197-MS. doi:10.4043/25197-MS

Kolk, H. J., Baaijens, A. E. & Vergobbi, P. (2005) Results from axial load tests on pipe piles in very dense sands: the EURIPIDES JIP. In: Proceedings of the 1st International

Accepted manuscript doi: 10.1680/jgeot.17.p.185

Symposium on Frontiers in Offshore Geotechnics (ISFOG), Perth, Western Australia:

Taylor & Francis, 661-667.

König, F. & Grabe, J. (2006) Time dependant increase of the bearing capacity of displacement piles. In: Piling and Deep Foundations. Conference Proceedings, DFI EFFC, Amsterdam, 709-717.

Kuwano, R. (1999) The stiffness and yielding anisotropy of sand. PhD thesis, Imperial College, University of London.

Lehane, B. (1992) Experimental investigations of pile behaviour using instrumented field piles, PhD thesis Imperial College London, University of London.

Lehane, B. M., Jardine, R. J., Bond, A. J. & Frank, R. (1993) Mechanisms of shaft friction from instrumented pile tests. *Journal of Geotechnical Engineering, ASCE*, 119(1), 19-35.

Lehane, B. M., Schneider, J. A. & Xu, X. (2005a) The UWA-05 method for prediction of axial capacity of driven piles in sand. In: *Proceedings of the 1st International Symposium on Frontiers in Offshore Geotechnics (ISFOG), Perth, WA, Australia:* Taylor and Francis/Balkema, 683-689.

Lehane, B. M., Lim, J. K., Carotenuto, P., Nadim, F., Lacasse, S., Jardine, R. J. & van Dijk, B. F. J. (2017) Characteristics of Unified Databases for Driven Piles. In: *Offshore Site Investigation and Geotechnics, Proceedings of the 8th International Conference,* London, UK.

Lim, J. K. & Lehane, B. M. (2014) Characterisation of the effects of time on the shaft friction of displacement piles in sand. *Géotechnique*, 64(6), 476-485.

NGI (2009) Time Effects on Pile Capacity, Factual Report, Test Site Larvik. Report

20061251-00-244-R, Norwegian Geotechnical Institute: Norwegian Geotechnical Institute.

Overy, R. (2007) The use of ICP design methods for the foundations of nine platforms installed in the UK North Sea. In: Proceedings of the 6th International Conference of the Society for Underwater Technology, Offshore Site Investigation and Geotechnics (SUT-OSIG), London, U.K., 359-366.

Prendergast, L. J., Gavin, K. & Doherty, P. (2015) An investigation into the effect of scour on the natural frequency of an offshore wind turbine. *Ocean Engineering*, 101(1), 1-11.

Rausche, F., Goble, G. G., and Likins, G. (1985) Dynamic determination of pile capacity. *Journal of the Geotechnical Division, ASCE*, 111(3), 367-383.

Rimoy, S. (2013) Ageing and axial cyclic loading studies of displacement piles in sands. PhD thesis, Imperial College London.

Rimoy, S. P. & Jardine, R. J. (2015) Axial capacity ageing trends of piles driven in silica sands. In: Proceedings of the 3rd International Symposium on Frontiers in Offshore Geotechnics (ISFOG), Oslo, Norway: Taylor and Francis Group. 1, 637-642.

Rimoy, S., Silva, M., Jardine, R. J., Yang, Z. X., Zhu, B. T., and Tsuha, C., T. C. H. (2015) Field and model investigations into the influence of age on axial capacity of displacement piles in silica sands. *Géotechnique*, 65(7), 576-589.

Samson, L. & Authier, J. (1986) Changes in pile capacity with time: Case histories. *Canadian Geotechnical Journal*, 23(1), 174-180.

Schmertmann, J. H. (1991) The mechanical aging of soils. *Journal of Geotechnical Engineering, ASCE*, 117(9), 1288-1330.

- Seidel, J. P., Haustorfer, I. J. & Plesiotis, S. (1988) Comparison of dynamic and static testing for piles founded into limestone. In: Proc. 3rd Int. Conf. App. Stress-Wave Theory to Piles, Ottawa, Canada, 717-723.
- Skov, R. & Denver, H. (1988) Time-Dependence of Bearing Capacity of Piles. In: Proc. 3rd Int. Conf. on App. of Stress-Waves to Piles, 879-888.
- Svinkin, M. R., Morgano, C. M. & Morvant, M. (1994) Pile capacity as a function of time in clayey and sandy soils. In: Proc. 5th Int. Conf. and Exhibition on Piling and Deep Foundations, Bruges, Belgium, DFI, Hawthorne, N.J, 1.11.1-1.11.8.
- Tan, S. L., Cuthbertson, J. & Kimmerling, R. E. (2004) Prediction of pile set-up in non-cohesive soils. In: Current practices and future trends in deep foundations, ASCE, Geotech. Special Pub. 125: 50-65.
- Tang, W.H., Woodford, D.L. and Pelletier, J.H. (1990) Performance reliability of offshore piles. Proc. 22nd Offshore Technology Conference; Houston, OTC 6379, pp 299-308. Angeles, California: ASCE Geotechnical Special Publication, 125, 50-65.
- Tavenas, F. & Audy, R. (1972) Limitations of the driving formulas for predicting the bearing capacities of piles in sand. Canadian Geotechnical Journal, 9(1), 47-62.
- Tsuha, C. H. C., Foray, P. Y., Jardine, R. J., Yang, Z. X., Silva, M. & Rimoy, S. (2012) Behaviour of displacement piles in sand under cyclic axial loading. Soils Foundations, 52(3), 393-410.
- White, D. J. & Zhao, Y. (2006) A model-scale investigation into 'set-up' of displacement piles in sand. In: In Physical modelling in geotechnics-6th ICPMG '06: London, UK: Taylor & Francis, 2, 889-894.

- Yang, Z. X., Jardine, R. J., Zhu, B. T., Foray, P., and Tsuha, C. H. C. (2010) Sand grain crushing and interface shearing during displacement pile installation in sand, *Géotechnique*, 60(6), 469-482.
- Yang, Z. X., Jardine, R. J., Zhu, B. T. & Rimoy, S. P. (2014) Stresses developed around displacement piles penetration in sand. *Journal of Geotechnical and Geoenvironmental Engineering, ASCE*, 140(3), 04013027.
- Yang, Z. X., Guo, W. B., Jardine, R. J. & Chow, F. (2017) Design method reliability assessment from an extended database of axial load tests on piles driven in sand. *Canadian Geotechnical Journal*, 54, 59-74.
- York, D. L., Brusey, W. G., Clemente, E. M., and Law, S. K. (1994) Set-up and relaxation in glacial sand. *J. of Geotech. Eng, ASCE*, 120(9), 1498-1513.
- Zai, J. (1988) Pile dynamic testing experience in Shanghai. In: *Proc. 3rd Int. Conf. on App. of Stress-Waves to Piles*, Ottawa, Canada, 781-792.
- Zdravković, L., et al. (2018) Ground characterisation for PISA pile testing and analysis, Zdravković, L., Jardine, R.J., Taborda D.M.G., Burd, H.J., Byrne, B.W., Gavin, K., Houlsby, G.T., Igoe, D., Liu, T, Martin, C.M., McAdam, R.A., Muir Wood, A., Potts, D.M., Skov Grethlund, J. and Ushev., E. (2018) Accepted for *Geotechnique*
- Zhang, C., Yang, Z. X., Nguyen, G. D., Jardine, R. J. & Einav, I. (2014) Theoretical breakage mechanics and experimental assessment of stresses surrounding piles penetrating into dense silica sand. *Géotechnique letters*, 4, 11-16.

Table 1. Meteorological data published for the locations nearest the three sites

Site	Rainfall	Temperature		Humidity	
	Annual	Monthly averages		Monthly averages	
	(mm)	Min (°C)	Max (°C)	Min (%)	Max (%)
Blessington (Dublin, Ireland)	734	5	16	73	83
Dunkirk (France)	710	4	18	78	84
Larvik (Norway)	763	2	16	60	85

Table 2 Summary of soil parameters and ground conditions for three test sites

	Unit	Larvik ⁽¹⁾	Dunkirk	Blessington
Water table BGL	m	2.2	5.4	13
Description		Loose to medium dense silty fine to medium sand with some silt layers.	Dense to very dense sand	Dense, medium to fine sand
Origin		Fluvial	Marine hydraulic fill	Glacial
Unit weight (γ_{bulk})	kN/m ³	18.9-19.6	17.1 ⁽²⁾	20.0 ⁽³⁾
Water content	%	26.5	5-7	10 ⁽³⁾
Relative density (D_r)	%	~20	100	100
Saturation (S_r)	%	100*	25-40*	60*
D_{90}	mm	0.37-0.8	0.4	0.6
D_{50}	mm	0.16-0.38	0.26	0.1-0.15 ⁽³⁾
Fines < 0.063 mm	%	6-20	0	5-10
Effective peak ϕ'_p (triaxial) and test conditions	°	36 ⁽⁶⁾ , $\sigma'_3 = 200$ kPa $e_0 = 0.80$ $D_r = 45\%$ (estimated)	37 ⁽⁷⁾ , $\sigma'_3 = 200$ kPa $e_0 = 0.64$ $D_r = 75\%$	42 ⁽⁵⁾ , $\sigma'_3 = 200$ kPa $e_0 = 0.59$ $D_r = 100\%$ (estimated)
Constant volume ϕ'_{cv} , (triaxial)	°	35 ⁽⁶⁾ , $\sigma'_3 = 200$ kPa	32 ⁽⁷⁾ , $\sigma'_3 = 200$ kPa	35 ⁽⁵⁾ , $\sigma'_3 = 200$ kPa
Constant volume interface shear δ_{cv} and test conditions	°	27.8 ⁽⁶⁾ , $\sigma'_n = 200$ kPa	27.5 ⁽⁶⁾ , $\sigma'_n = 200$ kPa	29.4 ⁽⁶⁾ , $\sigma'_n = 200$ kPa
Over consolidation ratios (OCR)		1	1	15 at 1m ⁽⁴⁾ 5 at 5m ⁽⁴⁾
Average q_c	MPa	2	30	15 ⁽⁵⁾
Average f_s	MPa	0.02	0.1-0.3	0.16 ⁽⁵⁾
Small strain stiffness value, G_{max}	MPa	-	50-130 ⁽⁸⁾	50-150 ⁽⁵⁾

¹NGI (2009), ²Chow et al. (1998) and Chow (1997), ³Gavin and O'Kelly (2007), ⁴Doherty et al. (2012), ⁵Prendergast et al. (2015), ⁶2017-18 triaxial and interface ring shear tests at Imperial College. Interface shear tests conducted against mild steel interfaces with R_{CLA} 8 to 13 μ m, following Jardine et al (2005) procedures, ⁷After Aghakouchak et al. (2015), ⁸Zdravković, L., et al. (2018). *Nominal as S_r varies with time and depth.

Table 3 Chemical tests on sand samples from the three sites

	pH	Sulfate (SO₄)	Carbonate (CO₃)	Total inorganic carbon	Conductivity
	-	mg/kg TS	% TS	% TS	mS/m
Dunkirk	8.6	1,000	9.5	1.9	8.3
Larvik	3.5	11,900	0.1	0.02	67.7
Blessington	8.0	<1,000	20.5	4.1	8.6

Table 4 Properties of piles

		Larvik	Dunkirk	Blessington
R _{cla} fresh MS**	µm	-	¹⁾ 1-3 ²⁾ ≈10 after extraction*†	-
R _{cla} pre-corroded MS	µm	¹⁾ NA ²⁾ 9.2 ³⁾ 8.5	¹⁾ ≈10* ²⁾ ≈10 after extraction *†	¹⁾ ≈10*
R _{cla} SS/GS	µm	-	¹⁾ 1-3 ²⁾ ≈1-3 after extraction*	¹⁾ ≈10*
R _{cla} air-abraded SS	µm	¹⁾ NA ²⁾ 10.3 ³⁾ 9.8	¹⁾ ≈1-3* ²⁾ ≈1-3 after extraction*	-
Grade MS	-	EN 10305-3, E220+CR2 - S2	E470	NA
Grade SS/GS	-	AISI 304	316L	NA
Outside diameter	mm	50-MS 48.2-SS	51-MS 50.6-SS	60
Wall thickness (t)	mm	2	8-MS 7.5-SS	4
D/t ratio	-	24-25	6.3-6.7	15
Contact length average	m	2.4	1.97	1.75

MS: mild steel, SS: stainless steel, GS: galvanised steel, NA: Not available, *estimated, †sand adhered to pile, **the 'fresh' interfaces were as delivered to site without any deliberate pre-corrosion or further air abrasion.

Measured centre-line average roughness (R_{cla}): ¹⁾ prior to installation, ²⁾ as found on extraction post tension test, including any in-situ corrosion and ³⁾ as found on spare not installed piles left exposed over 1yr on site.

Table 5 (a) Peak pile capacities for Larvik

File ID	Time (days)	Capacity (kN)	Pile	Driving energy	Plug length ratio (PLR)
P05	1	2.60	MS ¹	Variable	0.29
P04	14	3.71	MS ¹	Variable	0.52
P12	14	4.26	MS ¹	Variable	0.32
P02	78	3.94	MS ¹	Variable	0.42
P07	189	4.74	MS ¹	Variable	0.43
P03	313	5.45	MS ¹	Variable	0.40
P06	315	5.96	MS ¹	Variable	0.42
P08	696	5.45	MS ¹	Variable	0.54
P09	21	2.66	SS ²	Variable	0.60
P10	314	2.43	SS ²	Variable	0.54

¹ pre-corroded; ² air abraded. Failure defined at peak.

Table 5(b) Peak pile capacities for Dunkirk

File ID	Time (days)	Capacity (kN)	Pile	Driving energy	Plug length ratio (PLR)
S1	0.1	28.6	MS ¹	SPT	0.43
S2	2	29.7	MS ¹	SPT	0.52
S3	16	62.6	MS ¹	SPT	0.43
S4	16	59.3	MS ¹	SPT	0.36
S5	30	56.7	MS ¹	SPT	0.38
S6	92	67.4	MS ¹	SPT	0.41
S7+	93	64.2	MS ¹	SPT	0.41
S8	175	70.6	MS ¹	SPT	0.43
S9	274	71.1	MS ¹	SPT	0.38
S10B	315	71.7	MS ¹	Variable	0.46
S11	315	67.6	MS ¹	Variable	0.50
S12	273	79.6	MS ¹	Variable	0.49
S13+	273	76.7	MS ¹	Variable	0.40
S14+	176	73.9	MS ¹	Variable	0.48
S15	174	78.2	MS ¹	Variable	0.49
S16	90	71.6	MS ¹	Variable	0.40
S17	28	66.5	MS ¹	Variable	0.42
S18	14	67.8	MS ¹	Variable	0.43
S19	1	32.8	MS ¹	Variable	0.38
S20	0.1	31.2	MS ¹	Variable	0.36
R1	1	50.2	MS ^{2*}	Variable	0.22
R2	85	89.0	MS ^{2*}	Variable	0.21
R3	183	66.3	MS ^{2*}	Variable	0.24
R4	223	76.3	MS ^{2*}	Variable	0.23
S21-Inox	0.1	25.9	SS	Variable	0.38
S23-Inox	14	25.8	SS	Variable	0.44
S27-Inox	28	24.6	SS	Variable	0.43
S29-Inox	91	27.6	SS	Variable	0.44
RI5	1	32.3	SS ^{3*}	Variable	0.38
RI6	99	25.6	SS ^{3*}	Variable	0.38

¹fresh, ²pre-corroded, ³air-abraded, *Pile was used previously in this study as fresh MS or SS. SPT: as Standard Penetration Test, delivering up to 475 Joules/blow with 60-70% Energy Rating. Failure defined at peak.

Table 5(c) Pile capacities for Blessington

File ID	Time (days)	Capacity (kN)	Pile	Driving energy	Plug length ratio (PLR)
MS4	2	54.3	MS ¹	Variable	0.35
MS3	21	55.8	MS ¹	Variable	0.39
MS2	78	50.3	MS ¹	Variable	0.34
MS1	121	-	MS ¹	Variable	0.45
GS4	2	52.8	GS	Variable	0.21
GS3	21	50.3	GS	Variable	0.22
GS2	78	56.8	GS	Variable	0.23
GS1B	121	-	GS	Variable	0.19

¹pre-corroded. Failure defined at peak.

Table 6 Parameters and pile tension capacity predictions based on average of all CPTs

Site	δ_{cv}	β (API)	D ₅₀	R _{cla}	ICP*	API	NGI
	Deg	-	mm	μm	kN	kN	kN
Larvik	27.8	0.21	0.25	8.5	11.2 (85%)	4.4**	2.2
Dunkirk ¹	27.5	0.56	0.26	10.0	30.1 (47%)	5.1	27.9
Dunkirk ²	27.5	0.56	0.26	2.0	18.9 (15%)	5.1	27.9
Blessington	29.4	0.46	0.15	10.0	27.0 (52%)	7.2	27.5

¹Pre-corroded MS piles and fresh MS > 10 days, ² fresh MS < 10 day, air-abraded SS and SS
*ICP: values in parenthesis correspond to ratio of the capacity component term $\Delta\sigma'_{rd} \times \tan(\delta_{cv})$ to the total calculated capacity.

**API: The Larvik analysis applies API (1993) as API (2011) does not apply to loose sands

Table 7 Tension capacity analysis for MS piles: measured-to-calculated ratios for three methods

Site (days)	Day	Capacity measured*			ICP-05			API			NGI-05		
		kN			Q_{sm}/Q_{sc}			Q_{sm}/Q_{sc}			Q_{sm}/Q_{sc}		
		Larvik	Dunkirk	Blessington	Larvik	Dunkirk	Blessington	Larvik	Dunkirk	Blessington	Larvik	Dunkirk	Blessington
Pre-corroded	1-2	2.6	50	55	0.23	1.67	2.02	0.59	9.80	7.64	1.18	1.79	2.00
Fresh	1-2	-	33	-	-	1.75	-	-	6.47	-	-	1.18	-
Pre-corroded	85-100	4.2	89	56	0.38	2.96	2.07	0.95	17.5	7.78	1.91	3.20	2.04
Fresh	85-100	-	68	-	-	2.26	-	-	13.3	-	-	2.44	-
Pre-corroded	175-315	5.4	71	-	0.48	2.36	-	1.23	13.9	-	2.45	2.54	-
Fresh	175-315	-	74	-	-	2.46	-	-	14.5	-	-	2.65	-

Note: *average values are presented for the range of days considered for each set of pile types and site.

List of figures

Figure 1 Static tension capacity–time trends from first-time tests on steel piles driven at three sand sites, normalised by ICP-05 tension capacities. IAC refers to Intact Ageing Characteristic, as defined by Rimoy et al. (2015).

Figure 2(a) Concrete driven piles total axial compression capacities

Figure 2(b) Steel driven piles total axial compression capacities

Figure 3 Grain size distribution for Larvik, Dunkirk and Blessington

Figure 4(a) q_c variation with depth at Larvik. '16 refers to CPT performed in 2016 and '06 refers to CPT performed in 2006 by Karlsrud et al. (2014), see also Figure 5

Figure 4(b) q_c variation with depth at Dunkirk

Figure 4(c) q_c variation with depth at Blessington

Figure 4(d) u_2 variation with depth at Larvik. '16 refers to CPT performed in 2016 and '06 refers to CPT performed in 2006, see also Figure 5

Figure 4(e) u_2 variation with depth at Dunkirk

Figure 4(f) Suction and G_{\max} variation with depth at Dunkirk

Figure 4(g) Suction and G_{\max} variation with depth at Blessington

Figure 5 Larvik site layout

Figure 6 Dunkirk site layout

Figure 7 Blessington site layout

Figure 8: (A.1) Larvik pre-corroded MS and stainless steel piles, before use November 2015, (A.2-A.4) Larvik extracted piles, pulled out October 2017, (B) Dunkirk pre-corroded pile before use, (C) Dunkirk fresh MS extracted pile, dug out and (D) Dunkirk oxidised sand taken from face of a MS pile after extraction

Figure 9 Larvik tension test set up

Figure 10(a) Dunkirk tension test set up

Figure 10(b) Close up of Dunkirk test set up

Figure 11 Blessington tension test set up

Figure 12(a) Total number of blows versus depth at Larvik

Figure 12(b) Total number of blows versus depth at Dunkirk (SPT and variable energy driving)

Figure 12(c) Total number of blows versus depth at Blessington

Figure 13(a) Tension load versus displacement for selected tests with 10% pile diameter marker at Larvik

Figure 13(b) Tension load versus displacement for selected tests with 10% pile diameter marker at Dunkirk

Figure 13(c) Tension load versus displacement for selected tests with 10% pile diameter marker at Blessington

Figure 14(a) Normalised ultimate tension shaft resistance based on peak pile capacity for pre-corroded pile $Q_s/Q_{s,t=1 \text{ day MS}}$ at Larvik

Figure 14(b) Normalised ultimate tension shaft resistance based on peak pile capacity for pre-corroded pile $Q_s/Q_{s,t=1 \text{ day MS}}$ Dunkirk

Figure 14(c) Normalised ultimate tension shaft resistance based on peak pile capacity for pre-corroded pile $Q_s/Q_{s,t=2 \text{ day MS}}$ at Blessington

Figure 15(a) Average shear stress with time, small and larger diameter piles at Larvik

Figure 15(b) Average shear stress with time, small and larger diameter piles at Dunkirk

Figure 15(c) Average shear stress with time, small and larger diameter piles at Blessington

Figure 16(a) Ageing trends of micro-piles and 508mm OD piles driven at Larvik, showing latters' updated Intact Ageing Characteristic.

Figure 16(b) Ageing trends of micro-piles and 457mm OD piles driven at Dunkirk, showing latters' updated Intact Ageing Characteristic.

Figure 16(c) Ageing trends of micro-piles and 340mm OD piles driven at Blessington, showing latters' updated Intact Ageing Characteristic.

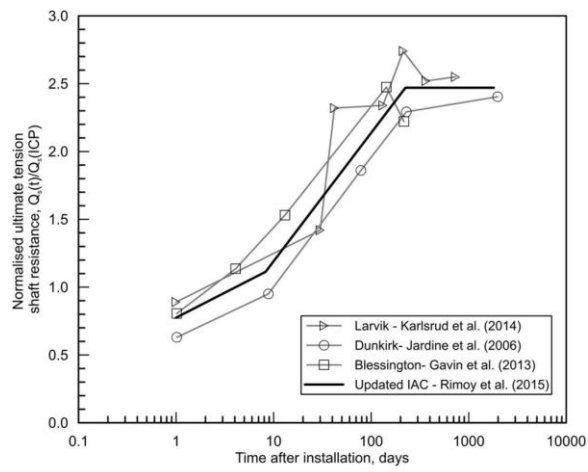


Fig1

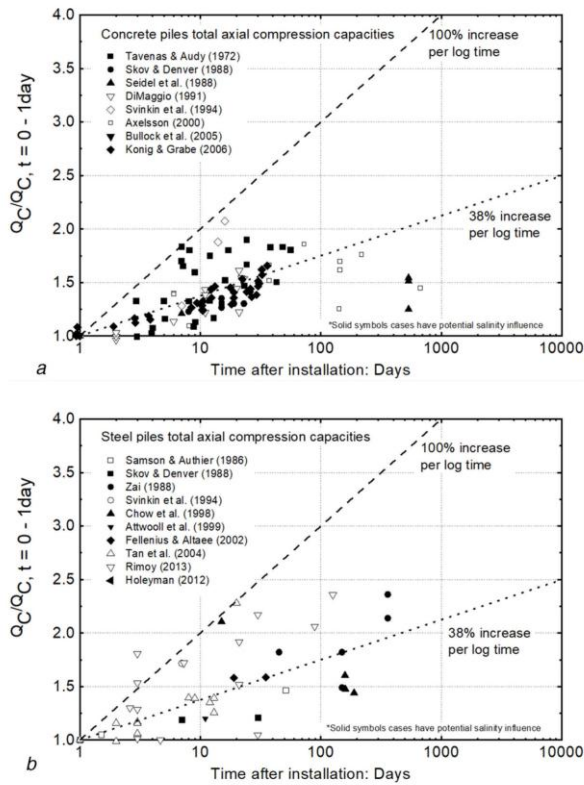


Fig2

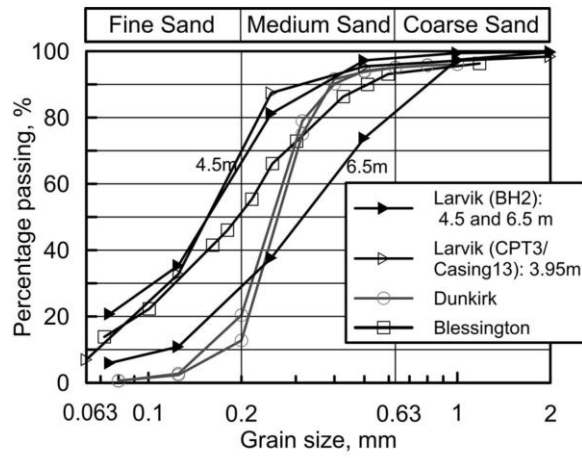


Fig3

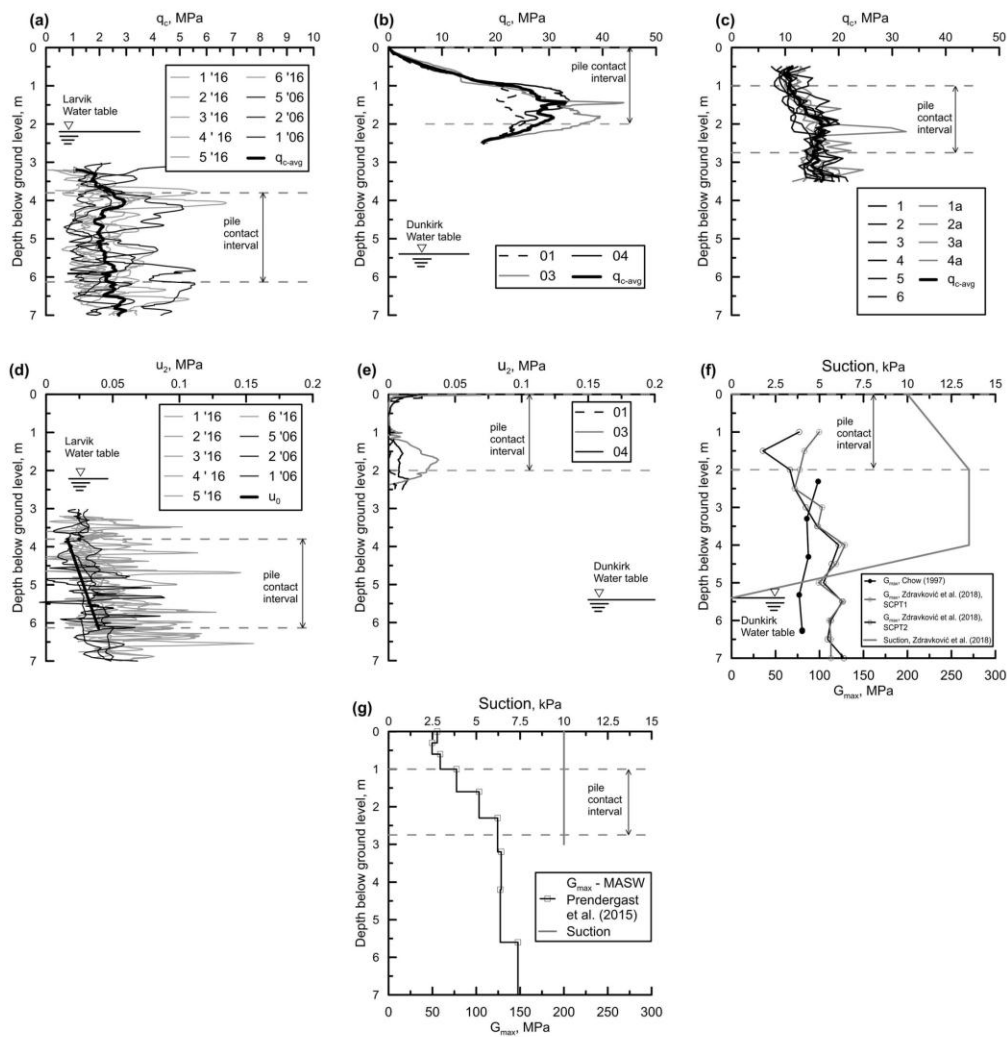


Fig4

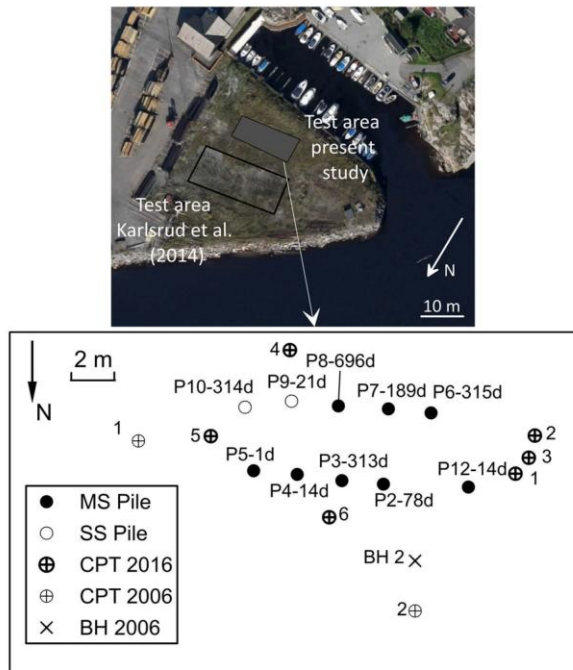


Fig5

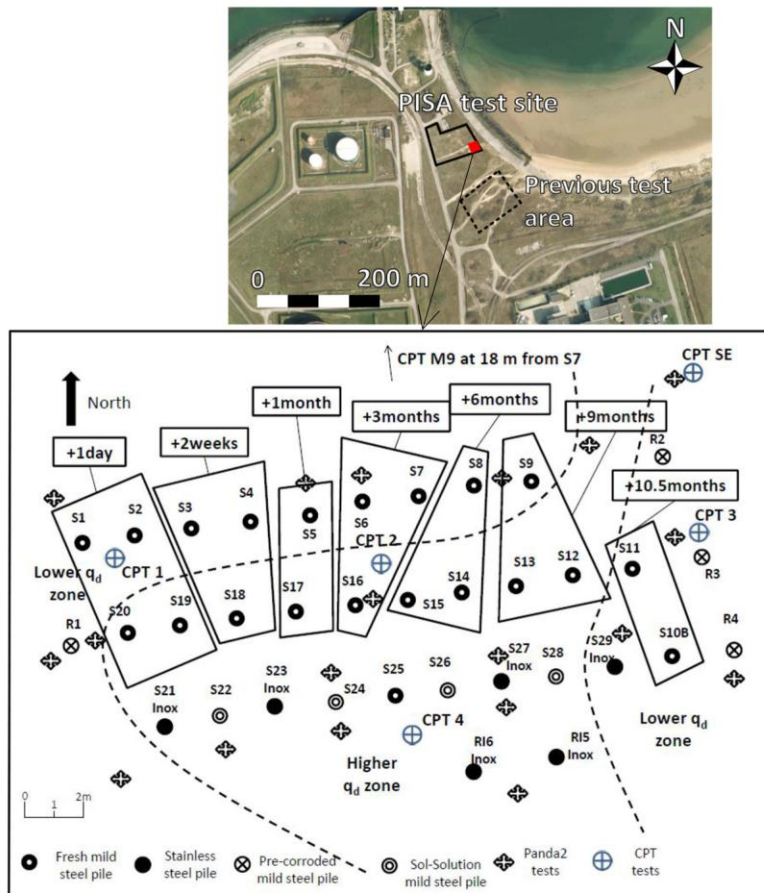


Fig6

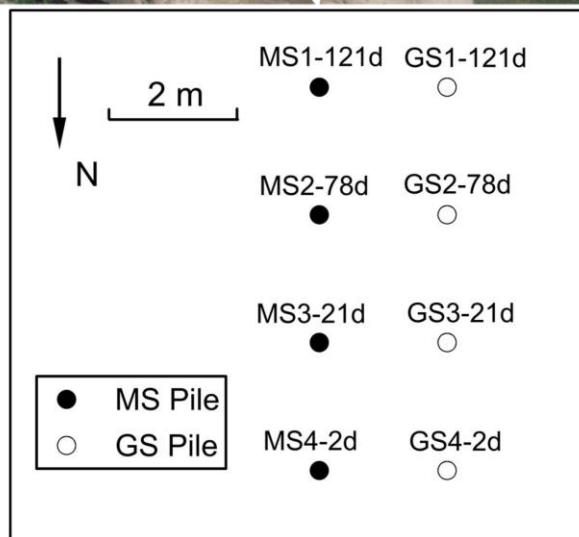
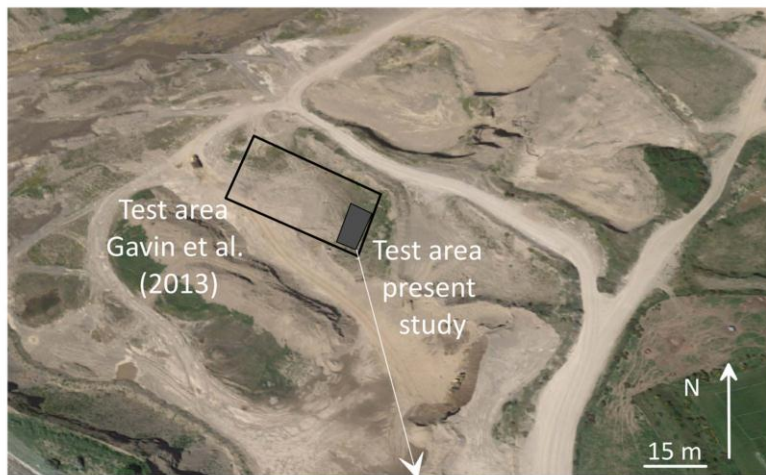


Fig7



Fig8

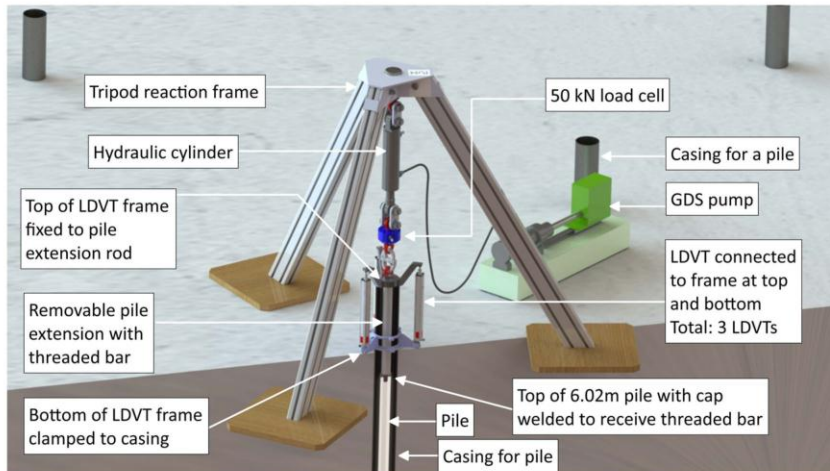


Fig9

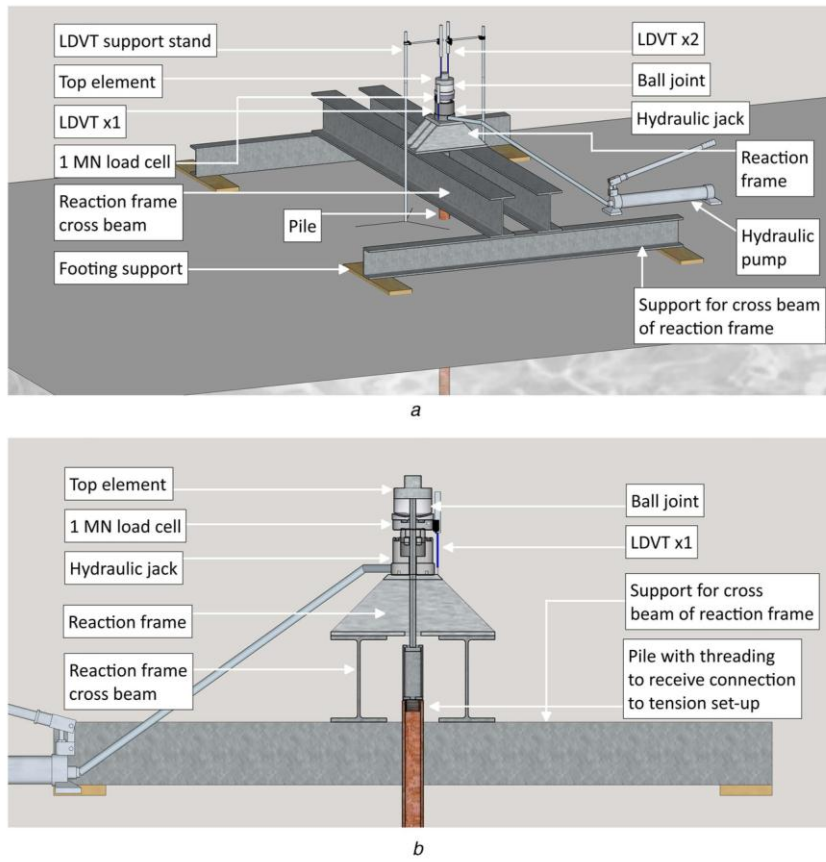


Fig10

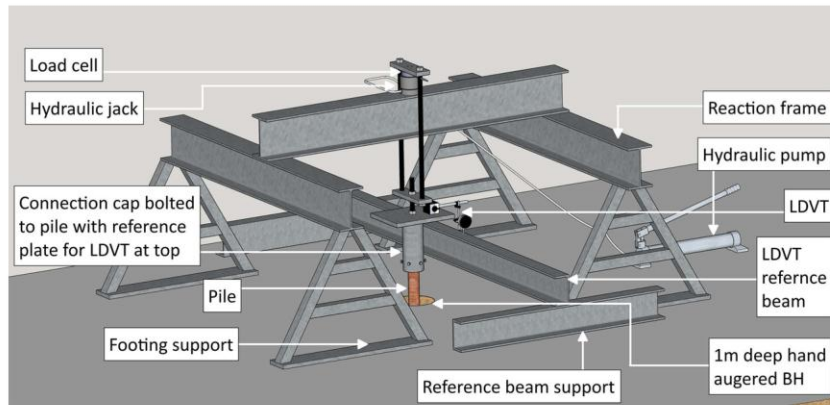


Fig11

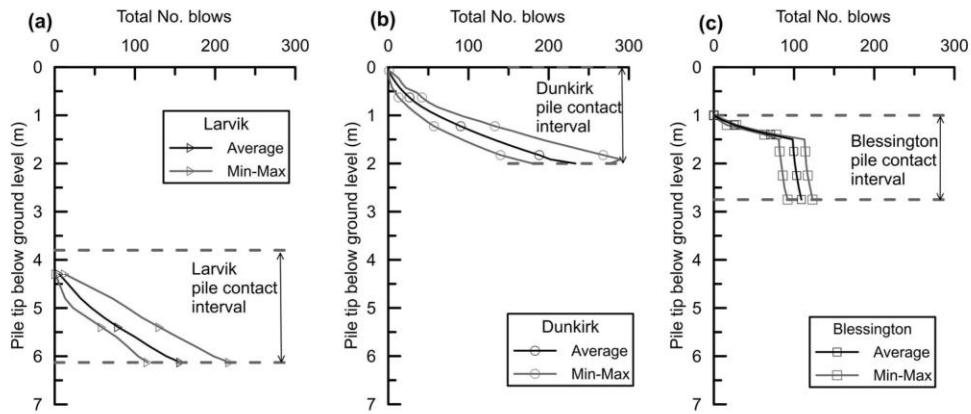


Fig12

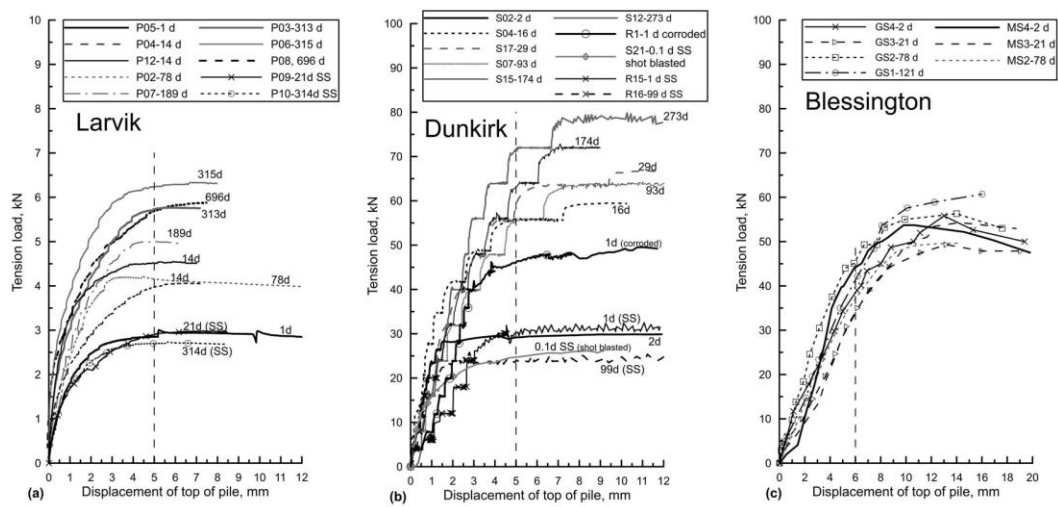


Fig13

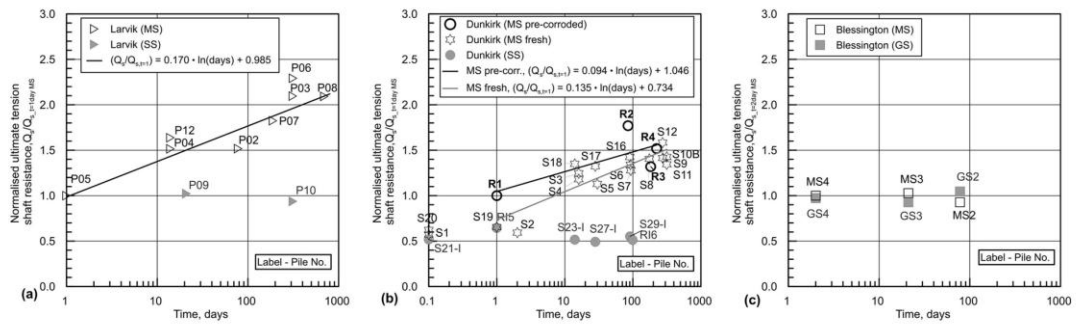


Fig14

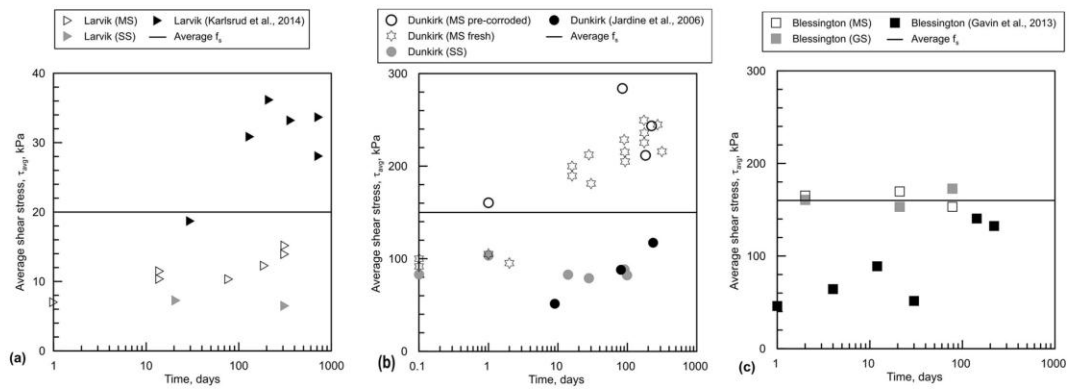


Fig15

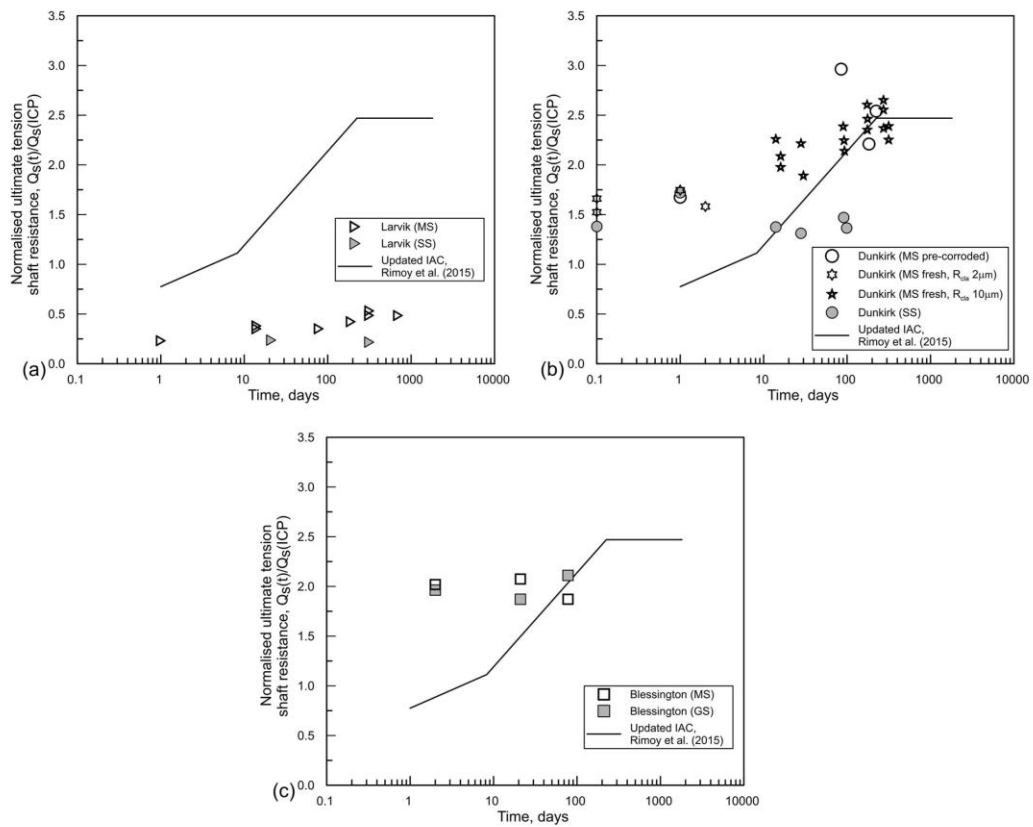


Fig16